CHAPTER ONE

INTRODUCTION

1.1 General Overview

Installation of Photovoltaic (PV) has been growing rapidly worldwide. Installation of PV generations maximum peak at Standard Test Conditions (STC) is increased from 7.5GW at 2007 to 70GW at the end of 2011. Many countries in the world trying for modest addition of the PV generation. Out of the total installation, Europe itself accounts for around 52GW generation; German leading is with 27GW of PV installation, followed by USA, Japan, Spain and China. Many large scale PV plant installations are in progress (E.g. 550MW Topaz plant and 500MW Blythe solar plant both in California…etc). Greece plans to add 10000MW before 2015. Studies show that world-wide installation of PV generation will reach above 1.8TW. As of now Golmud solar park (200MW) is the biggest individual solar plant in the world. PV cell converts light energy into electrical energy. Many PV cells connected in series will form PV cell string to achieve high voltage, and many strings are connected in parallel to increase the current capability will form a PV module or PV panel. PV cells generate Direct Current (DC) voltage and this DC voltage is converted into Alternating Current (AC) by using power electronics inverter. PV output is proportional to the light energy (irradiance), so there is a need for storage battery, to ensure supply during less sun irradiance (in night) hours. But this leads to a high cost and environmental pollution because of chemical substance in the battery. Also batteries have less life time. So grid connected PV systems have been very popular, PV system will inject all its power to the electrical grid, so PV system is fully utilized. Grid integration is must for MW size PV plants. Proper scheduling between PV and other conventional power plant can ensure full uninterruptible power supply [1].

1.2 Problem Statement

Photovoltaic generation improves power system reliability and power quality, but it leads to a problem related to power system stability and security during disturbances and abnormal conditions. So addition of these resources in the existing network opens up new challenges in power system protection due to its unpredictable nature and multi feed capability. In order to allow successful large scale penetration of PV cells in existing distribution network, this work has been done to investigate the nature of these problems.

1.3 Objectives

The main objectives of the thesis are:

- To study the performance of the grid connected photovoltaic system under various grid disturbances and climatic conditions such as three phase fault, voltage variation, frequency variation and sudden change in the irradiance.
- To analyze the impact of various PV system dynamic elements and controllers during abnormal conditions.

1.4 Methodology

The thesis is undertaken according to the following steps:

(1) Study and understand photovoltaic system.

(2) Construct the model of PV panel using MATLAB/SIMULINK.

(3) Study Maximum Power Point Tracker (MPPT) and Phase Locked Loop (PLL).

(4) Build the complete system including distribution system by using MATLAB/SIMULINK software.

(5) Evaluate the performance of the system under various conditions based on simulation results.

1.5 Thesis Layout

The thesis consist of five chapters. Chapter one gives an introduction to the thesis, including general overview, problem statement, objectives and methodology. Chapter two presents literature review of PV panel, modeling of PV panel, control strategy of grid tied inverter, phase locked loop and general protection issues in distributed generation. Chapter three shows the mathematical model of the PV system. Chapter four presents the simulation results under various conditions. Chapter five consist of conclusion and recommendations.

CHAPTER TWO
LITERATURE REVIEW

2.1 General Concepts

Photovoltaic is the direct conversion [2] of light into electricity at the atomic level. Some materials exhibit a property known as the photoelectric effect that causes them to absorb photons of light and release electrons. The photoelectric effect was first noted by a French physicist, Edmund Bequerel, in 1839, who found that certain materials would produce small amounts of electric current when exposed to light. In 1905, Albert Einstein described the nature of light and the photoelectric effect on which photovoltaic technology is based, for which he later won a Nobel prize in physics. The first photovoltaic module was built by Bell Laboratories in 1954. It was billed as a solar battery and it was mostly just a curiosity as it was too expensive to gain widespread use. In the 1960s, the space industry began to make the first serious use of the technology to provide power aboard spacecraft. Through the space programs, the technology was advanced, its reliability was established, and the cost began to decline. During the energy crisis in the 1970s, photovoltaic technology gained recognition as a source of power for non-space applications [3].

2.2 PV Principle

Solar cells are made out of a semiconductor material. Since light is the collection of small packets called quanta, and it is a electromagnetic wave. Light energy contains many photons, which move in different frequencies, each frequency in the lights spectrum, contains a specific energy $E=h\nu$. When PV material is exposed to light, some photons are reflected on the PV panel surface, remaining photons are absorbed by the PV material, depending on the on material property, the absorbed photon, which have energy greater than band gap energy of the semiconductor material (for Silicon (Si) energy gap is

1.12eV) generate free charge carriers in the semiconductor bulk. Due to band bending in p-n junction semiconductor, electrons try to move to lower energy level (n region) and holes try to move higher energy level (p region), so it creates a potential difference between p and n region. From the above we can say that voltage across the cell is dependent on the energy gap. Due to the generated voltage (across p-n junction) there will be current circulating inside the cell (diode forward bias) called dark current (since it is not directly related to irradiance). Figure 2.1 shows the operating region of PV p-n junction semiconductor devices [3]. From the Figure 2.1 it can be observed that PV cell has a non-linear V-I characteristics. Also it is depends on irradiance, temperature and other climatic condition as shown in the Figure 2.2.

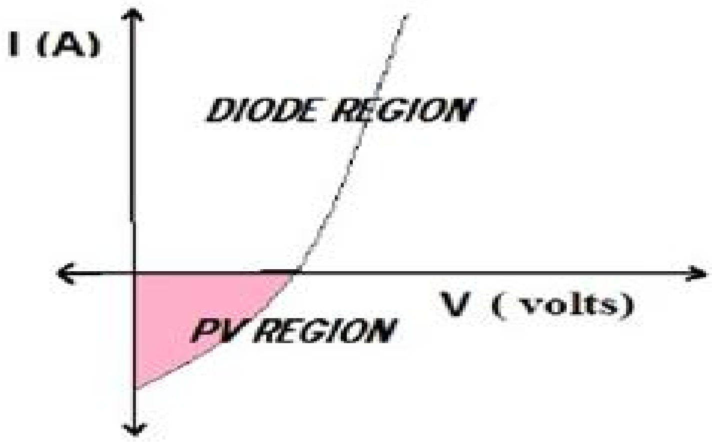

Figure 2.1: PV operating region

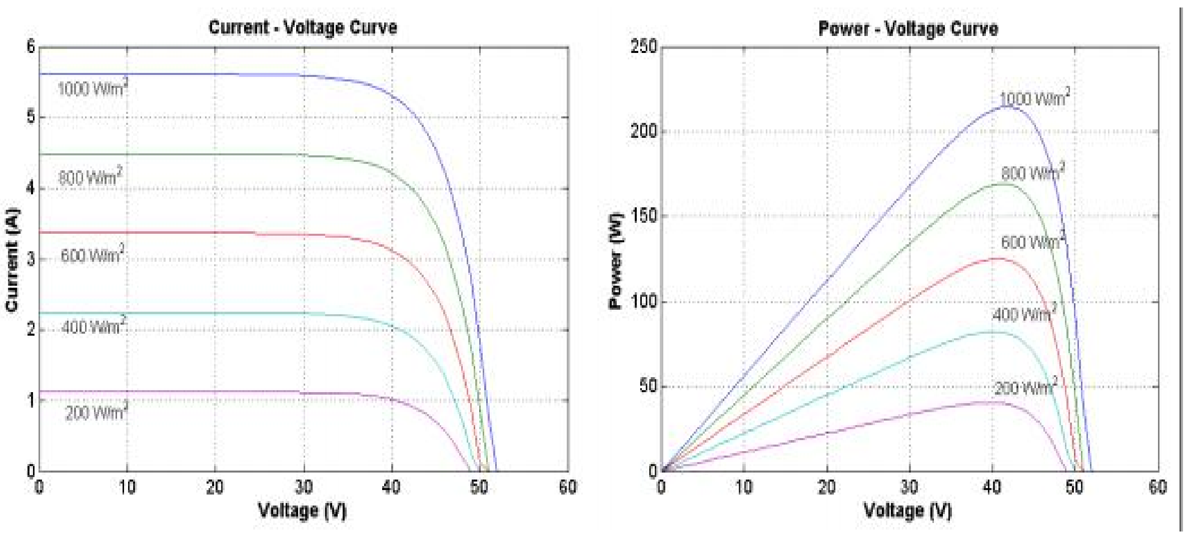

Figure 2.2: V-I and P-V Characteristics of Sanyo 215W PV Panel

2.3 Important Terms in PV Panel

PV output voltage and current depends on [4] temperature and irradiance. Power generated by PV panel is proportional to irradiance. Also there are other important parameters which are considered for the design of PV panel are explained in this section.

2.3.1 Irradiance

The radiation of the sun reaching the earth is distributed over a range of wavelengths from 300nm to 4 micron approximately, which is partly reflected by the atmosphere and partly transmitted to the earth's surface. Photovoltaic applications used for space, such as satellites or spacecraft, have sun radiation availability different from that of PV applications at the earth's surface. The radiation outside the atmosphere is distributed along the different wavelengths in a similar fashion to the radiation of a black body at temperature 5762K following Plancks law, whereas at the surface of the earth, the atmosphere (e.g. ozone layer which filter Ultra Vilot (UV) light) selectively absorbs the radiation at certain wavelengths. It is common practice to distinguish two different sun spectral distributions:

• Air mass spectrum- AM0

Spectrum outside the earth's atmosphere on a plane is perpendicular to the sun at the mean earth-sun distance. The power density outside the earth's atmosphere is 1367W/m^2 and this is known as the solar constant.

• Air mass spectrum - AM1.5

Air mass refers to the relative path length of the direct solar beam through the atmosphere. The path of the light through the atmosphere is shortest when the sun is at its zenith (perpendicular to the earth's surface), the path length is 1.0 (AM 1.0) and this gives rise to the AM1 spectrum. Obviously, the sun is not always at the zenith. When the angle of the sun from zenith increases, the air mass increases so that at an angle of 48.2^o the air mass is 1.5(refer Figure2.3).

This has been adopted as the standard sunlight spectrum for terrestrial arrays for actual spectrum [3].

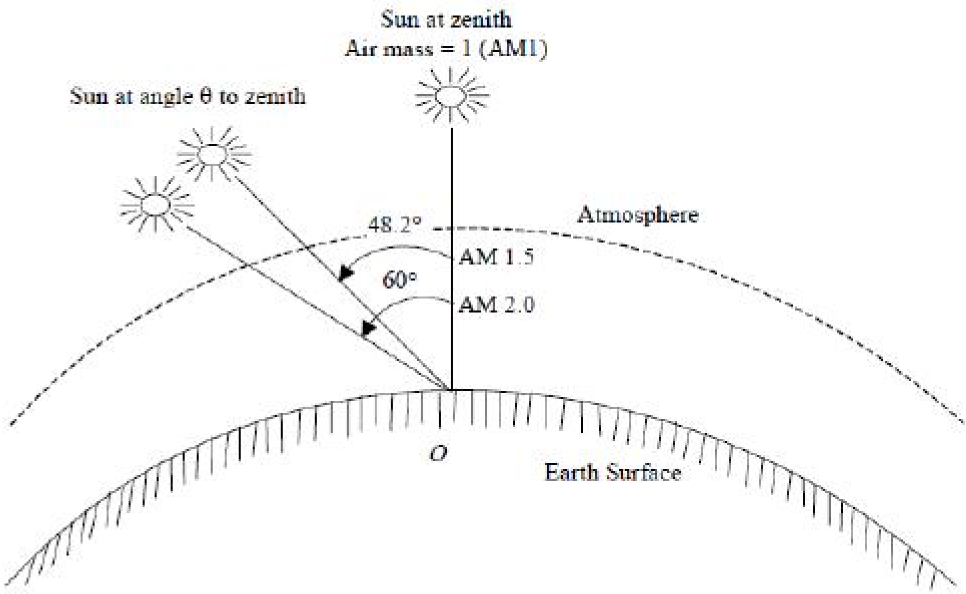

Figure 2.3: Concept of air mass spectrum

Important terminology to express magnitude of solar light:

• Spectral irradiance I_{λ}: Power received by a unit surface area in a wavelength differential dλ, the units are W/m^2 µm.

• Irradiance: The integral of the spectral irradiance extended to all wavelengths of interest and the units are W/m^2.

• Radiation/Insulation: The time integral of the irradiance extended over a given period of time, therefore radiation units are units of energy is given in kWh/m^2–day, or simply electrical units per day.

2.3.2 Temperature

PV output will change with respect to temperature, because band gap, carrier concentration are dependent on temperature. For maximum power output of the module, it is needed to lower operating temperatures but increase the irradiance. The typical temperature coefficient of power is 0.5%/^{o}C for mono or polycrystalline silicon cells. The cell temperature of open rack modules (e.g. a-Si), however, is governed by several external factors such as ambient temperature, irradiance level, wind speed, wind direction, and tilt angle of the module in the array. Temperature considered is actually the PV cell temperature and not its temperature of the rack or atmospheric temperature. As per standard PV cell outputs, are given in cell temperature of 25^o.

2.3.3 Nominal operating cell temperature

Nominal Operating Cell Temperature (NOCT) is the cell temperature, when open circuited panel subjected to an irradiance of $800W/m^2$, ambient temperature of 20^oC and wind speed of 1m/s at a module tilt angle 45^o. This will give the idea of cell temperature rise in the PV panel. Nominal value of NOCT will be around $43^o - 50^o$ C. This information is available in the manufacturing data sheet. NOCT temperature given in data sheet will be useful to find approximate PV panel temperature using known ambient temperature.

$$T_c = \frac{(T_{NOCT} - T_a)xE}{800} \qquad (2.1)$$

Where T_C =cell temperature, T_{NOCT}=ambient temperature, T_a= air temperature and E=irradiance.

2.3.4 Standard test conditions

The STC (also known as Standard Reporting Conditions (SRC)) is defined with nominal cell temperature 25^oC, nominal irradiance level $1000W/m^2$ at spectral distribution of air mass 1.5 solar spectral content. Many of the important parameter given in the data sheet is based on this condition.

2.3.5 Open circuit voltage

Voltage across the PV panel, when it is open circuited (I_{PV}= 0). This voltage will change with respect to irradiance and temperature. The open circuit voltage (V_{oc}) will increase with respect to irradiance, decrease with respect to temperature (-ve coefficient τ_v). This is the important parameter of PV panel, which is used to calculate maximum PV voltage and important for system design. Both V_{oc} and τ_v are given in the manufacturer data sheet at STC. All points lie in the x-axis as shown in Figure 2.2 are open circuit voltages with respect to different irradiance.

2.3.6 Short circuit current

Current supplied by PV panel when its terminals are shorted. This current will change with respect to irradiance and temperature. The short circuit current (I_{sc}) will proportionally increase with respect to irradiance, logarithmically increase with respect to temperature (+ ve coefficient τ_i). This is the important parameter of PV panel and is used to calculate maximum fault current, it is also important for system design. Both (I_{sc}) and (τ_i) are given in the manufacturer data sheet at STC. All points lie in the y-axis as shown in Figure 2.2 are short circuit currents with respect to different irradiance.

2.3.7 Maximum power point

As shown in the Figure 2.2 PV voltage and currents are nonlinearly related, so at a particular voltage, PV panel supplies maximum power, that in-turn changes with respect to climatic conditions (e.g. irradiance, temperature...etc). The point (voltage, current) in Figure 2.2 at which PV panel supplies maximum power is called Maximum Power Point (MPP). So to operate PV at MPP requires separate controller called (MPPT). MPPT will play an important role in PV system dynamics.

2.3.8 Maximum power voltage and current

Voltage and current of the PV panel, when it is operating in maximum power point are called maximum power voltage (V_m) and current (I_m). Values of ($V_m$and I_m) are given in the data sheet at STC.

2.3.9 Fill factor

Every cell has a life expectancy. As time progresses, the quality of cell goes down. Hence, it is essential to check the quality [4], periodically so that it can be discarded once the quality falls below certain level. The quality of the cell called Fill Factor (FF) which can be calculated as:

$$FF=\frac{I_m \times V_m}{V_{oc} \times I_{sc}} \tag{2.2}$$

Ideally, the Fill factor should be 1 or 100%. However, the actual value of FF is about 0.8 or 80%. A good panel has fill factor in the range of 0.7 to 0.8. For a bad panel it may be as low as 0.4.

2.3.10 Temperature coefficient

Temperature co-efficient (τ_v V/^{o}C and τ_i A/^{o}C) given in the PV panel data sheet is used to quantify change in the PV panel voltage and current with respect to temperature. This is very important to model a PV panel.

2.4 Manufacturer Data Sheet

To model the practical PV panel, its required to use only the data given in the manufacturer data sheet. Refer appendix (B) for the sample manufacturer data sheet. Clear understanding of the data given in the data sheet must for modeling of the PV panel. All the quantities are already explained above.

2.5 Modeling of PV Panel

PV panel modeling is very important for dynamic analysis of PV system.

2.5.1 Single diode model

Photovoltaic cell is made of simple p-n junction semiconductor [5]. But instead of external voltage excitation, light (photons) is used to excite the electrons and holes. And the voltage across the cell is depends on the energy gap. Due to the voltage across p-n junction, which forward biases the junction, there will be current circulating inside the cell called dark current (independent of irradiance). Hence PV is modeled as a current source parallel with a diode. Figure 2.4 shows the circuit diagram of single diode model.

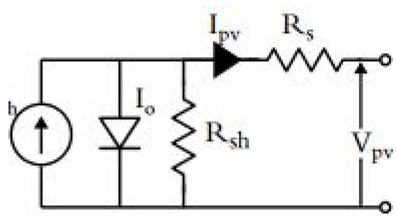

Figure 2.4: Single diode model

$$I_{pv} = I_{ph} - I_o\left[e^{\left(\frac{V+I_{pv}R_S}{V_T}\right)} - 1\right] - \left[\frac{V+I_{pv}R_S}{R_{sh}}\right] \quad (2.3)$$

$$V_T = \frac{nKT}{q} \quad (2.4)$$

Where I_{ph}=light generated current in the cell, I_o=saturation current, V_T=thermal voltage, k=Boltzmann's constant, R_s=series resistance, R_{sh}=shunt resistance, q=elementary charge($1.602x10^{-19}$ C) and n=diode ideality factor.

By neglecting R_s andR_{sh}, we have:

$$I_{pv} = I_{sc} - I_o\left[e^{\left(\frac{V}{V_T}\right)} - 1\right] \quad (2.5)$$

When $I_{ph} = 0$ then the open circuit voltage is:

$$V_{oc} = I_{sc} - V_T \ln\left[\frac{I_{sc}}{I_o} + 1\right] \quad (2.6)$$

When $V_{ph} = 0$, then:

$$I_{sc} = I_{pv} \quad (2.7)$$

From the above equation, open circuit voltage is logarithmically related with irradiance (PV panel photon current).

(a) Series resistance

The series resistive losses are present in practical solar cells. In fact, the current generated in the solar cell bulk travels towards the contacts through resistive semiconductor material, both in the base region (normally P type-not heavily doped) and in the narrow emitter region (N type), which are normally heavily doped. Besides these two components, the resistance of the metal grid, contacts and current collecting bus also contribute to the total series resistive losses. It is common practice to assume that these series losses can be represented by a lumped resistor (R_s) which is dependent on temperature is called the series resistance of the solar cell.

(b) Shunt resistance

A number of shunt resistive losses are identified, such as localized shorts at the emitter layer or perimeter shunts along cell borders are among the most common. This is represented generally by a lumped resistor (R_{sh}), in parallel with the intrinsic device.

2.5.2 Double diode model

In the above model, effect of non ohmic losses, due to recombination in the space charge region of the solar cell is not considered. This is relevant at low voltage bias and can be represented in an equivalent circuit by a second diode term with saturation current (I_{02}), which is different from the saturation current (I_0) of the ideal solar cell diode, and given ideality diode factor different from 1, normally diode with ideality factor 2 is used for this purpose. In practice, only few devices exhibit a totally ideal I(V) characteristic with ideality coefficient equal to unity, so it is common practice to also add a parameter n to account for non idealities in the dark current diode and the single diode model can be modified to take this effect into account. Figure 2.5 shows the circuit diagram of double diode model.

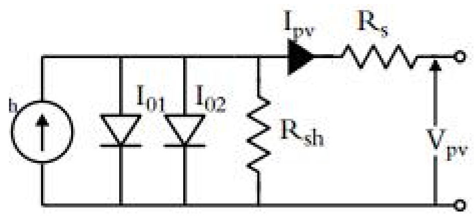

Figure 2.5: Double diode model

$$I_{pv} = I_{ph} - I_{01}\left[e^{\left(\frac{V_{pv}+I_{pv}R_s}{nV_T}\right)} - 1\right] - I_{02}\left[e^{\left(\frac{V_{pv}+I_{pv}R_s}{2V_T}\right)} - 1\right] - \left[\frac{V_{pv}+I_{pv}R_s}{R_{sh}}\right] \quad (2.8)$$

In Figure 2.5, first diode (I_0) with ideality factor n accounts for dark current (independent of irradiance) and second diode with a ideality factor accounts for non ohmic shunt losses in the solar cell. The some disadvantages of double diode model are:

• Many parameters (R_s, R_{sh}, I_{01}, I_{02}, I_{ph}, V_T) are not available, because it is depended on property of the material. Also there are not given by manufacturer.

• Semiconductor equations are derived from five carrier transport differential equations, which assume uniform doping and crystalline material. But this is not true in the case with practical module and thin film PV (which have p-i-n junction). So there is a need to model PV cell that uses only the information given by the manufacturer data sheet. Also it must take care of change due to climatic condition (normally irradiance, temperature and wind speed). Translation equations are proposed to translate voltage and current from one condition to another condition.

2.6 PV System Design

Many panels connected in series and parallel as shown in the Figure 2.6 for achieving high voltage and power [6].

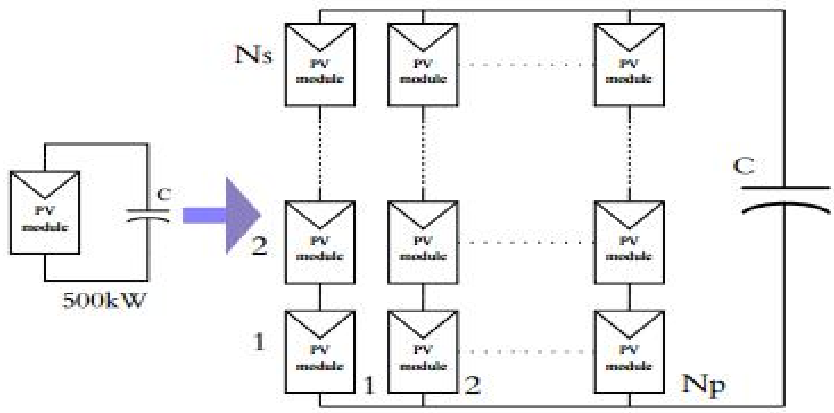

Figure 2.6: Structure of PV array

2.6.1 Selection of PV arrays

Figure 2.7 shows the PV System single line diagram.

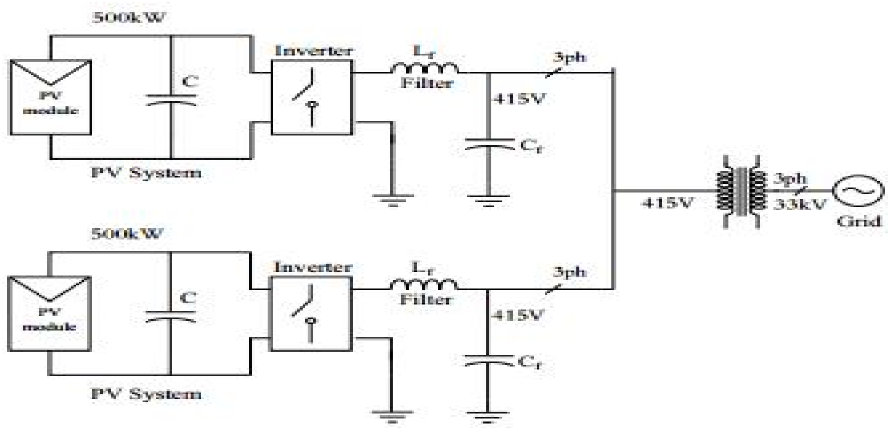

Figure 2.7: PV System single line diagram

Number of panels required is selected based on the calculation given below:

if $v_{grid} = v_{gm} \sin \omega t$

for UPF $i_s = I_{sm} \sin \omega t$

so $v_i = L_f \omega I_{sm} \cos \omega t + V_m \sin \omega t$

$$v_i = jX_L i_s + v_{grid} \tag{2.9}$$

Where v_i=inverter output voltage, L_f=filter inductance, X_L=inductive reactance, ω= grid frequency in rad/s, i_s=source current and v_{grid}=grid voltage. Required inverter voltage is decided by grid voltage and voltage across inductor as in above Equation. Also inverter voltage is depends on DC bus voltage (PV Voltage) and method of switching, maximum inverter voltage possible for Sine triangle Pulse Width Modulation (PWM) is V_i=V_{pv}/2. Maximum inverter output voltage required is calculated by assuming inductor voltage of 0.1pu, when rated current flow through the inductor, and 10% increase in grid voltage is considered

Required max $V_{imax} = 0.1v_{grid} + 1.1v_{grid}$

$$V_{pv\,min} = 2V_{i\,max} \tag{2.10}$$

It is required to connect many PV panels in series to achieve the voltage requirement of the inverter. To supply maximum possible power to the grid at all environmental condition, minimum PV voltage (less irradiance and high temperature) must be equal to two times of maximum required inverter voltage. For PCC line voltage of 415V, minimum of 20 SANYO 215A panels (N_s=20) have to be connected in series as shown in the Figure 2.11, so maximum possible voltage is equal to:

$N_s \times V_{oc}$= 51.3 × 20 = 1026V and minimum PV voltage is equal to:

$Ns \times V_{min}$ = 820 V.

To achieve the required power rating (normally represented in STC), many PV string must be connected in parallel, which are called as PV arrays.

$$N_p = \frac{P_{pv}}{N_s V_m} \tag{2.11}$$

For 500kW PV system N_p=117 PV string must be connected in parallel. So 500KW PV system needs 2340 SANYO 215A panels. Actual rating of PV system is equal to 504.18KW according to equation $P_{pv}=(N_s \times N_p)\cdot P_{panel}$.

2.6.2 Inverter

Since main focus is on studying transient response for large signal disturbances, so harmonics generated by the inverter is not of much interest. So average model of inverter is sufficient for the analysis, but simulation carried out for both systems with and without inverter shows no significant difference found.

The inverter design details as follow:

• Two level three phase inverter with the rating of 500KW.

• Sine triangle PWM with a switching frequency equal to5KHz.

• LC filter is used.

• Inverter is modeled as a first order system with the time constant equal to the half of switching time (bandwidth is equal to twice that of switching frequency).

• Constant current mode control is used to inject UPF power to the grid.

• Voltage controller is used to regulate the DC bus voltage.

2.6.3 Maximum power point tracking and DC-DC converter

The PV cells operate under varied environmental conditions and require control at its output terminal to extract maximum power from the system. This is done by a process called maximum power point tracking. There are several process of maximum power point tracking. Each technique has its own advantage and disadvantages. Some commonly used techniques are Incremental Conductance (IC) method, hill top, perturb and observe etc. Hohm and Ropp [7] performed a comparative study of various MPPT techniques using experimental method. The output of PV module changes with direction of sun, irradiance level and temperature. There is a single maximum power point in I-V characteristics of a PV module under a particular operating condition. It is desired that PV module operates close to the maximum power point which occurs at the knee point of I-V characteristics. For the purpose of research a DC–DC boost converter has been connected at the output of the PV panel. The MPPT controller determines the duty cycle of the boost converter to achieve the required extraction of power at maximum power point. Perturb and Observe (P and O) method has been be used in research for carrying out the MPPT. The flowchart for P and O algorithm is shown in Figure 2.8.

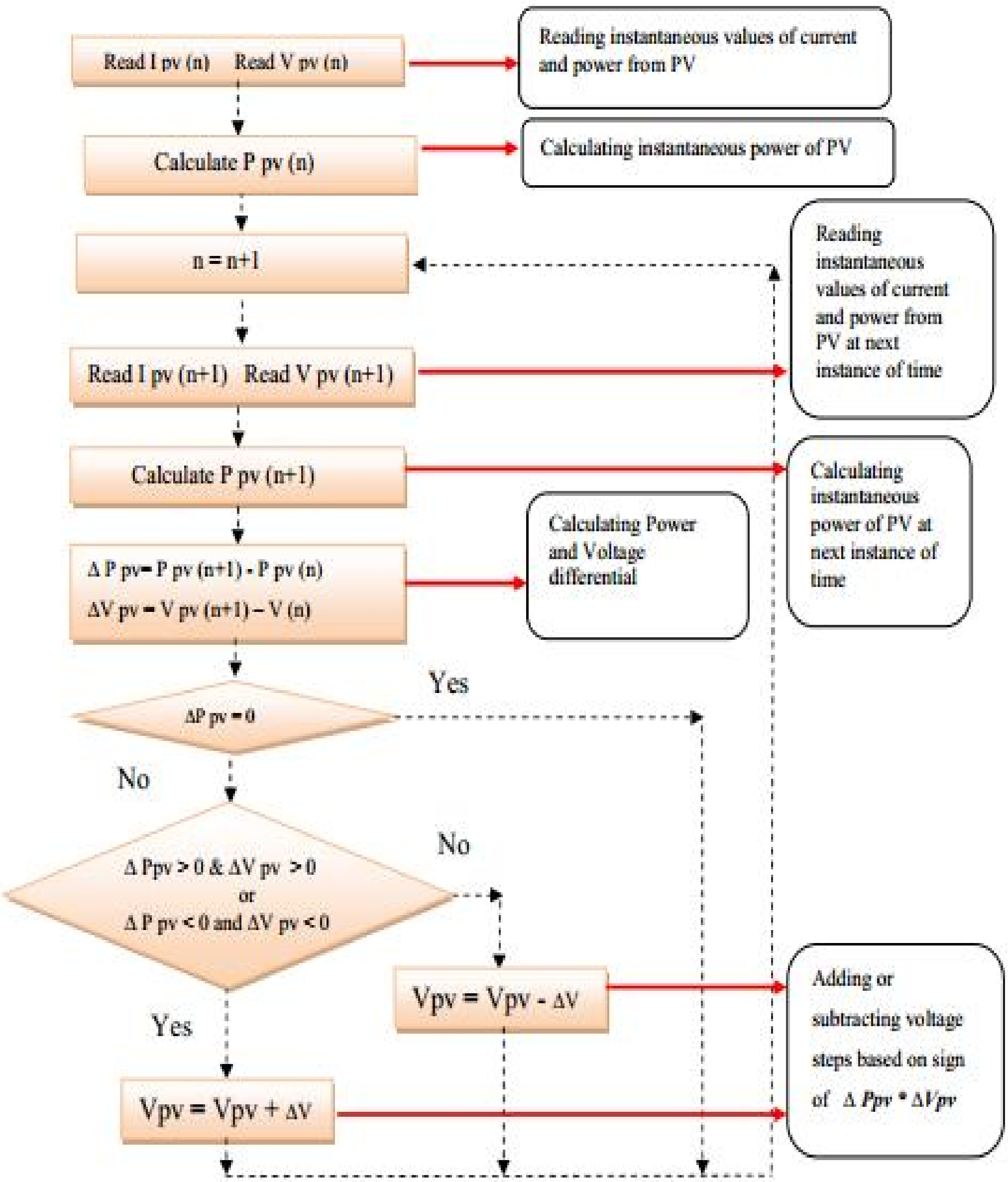

Figure 2.8: Flow-chart for P and O MPPT algorithm

Complete design procedure for DC-DC boost converter has been detailed below. Figure 2.9 is the circuit arrangement of a DC-DC boost converter. L and C outs are the boost converter inductance and capacitance. The capacitor C holds the voltage for the boost converter.

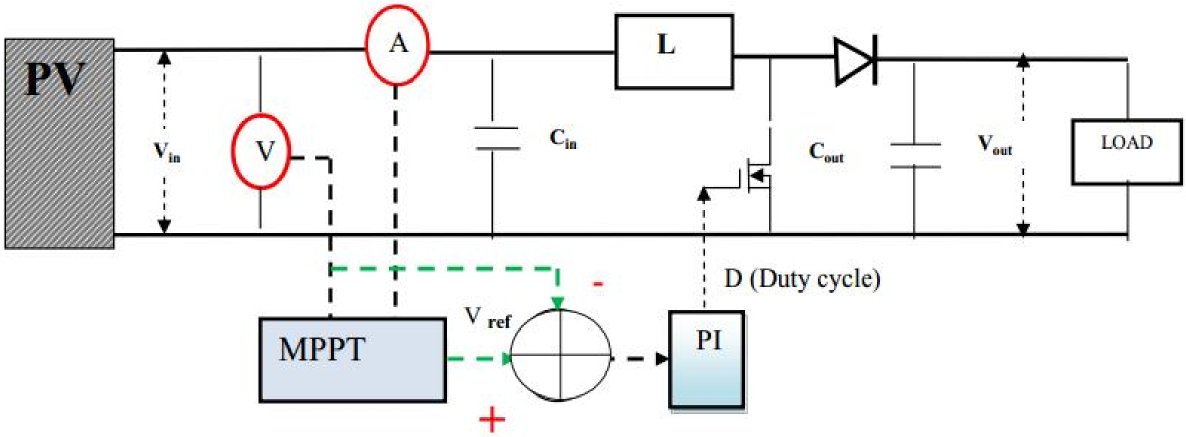

Figure 2.9: Block diagram for boost converter

2.7 Control Strategy of Grid Tied Inverter

For the purpose of control, grid is considered as a voltage source with infinite capacity controlling the output current of the inverter (PWM) algorithm of the grid connected inverter is based on a double closed loop current control as shown in Figure 2.10.

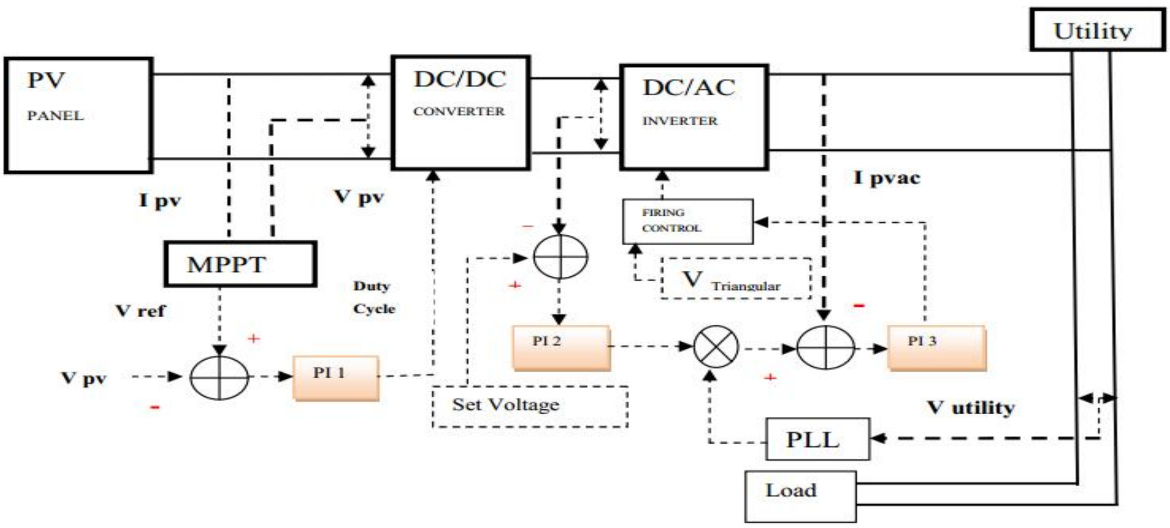

Figure 2.10: Block diagram-grid tied PV system control

The voltage loop is the outer loop and current loop is the inner loop. The outer loop functions to stabilize the DC voltage of the photovoltaic array. The aim of inner loop is to track the given current signal. PLL (Phase Locked Loop) is used to achieve the output current of the inverter such that it is in sinusoidal and in phase with utility voltage. The reference current produced by the voltage loop is multiplied by sinθ which is captured from PLL. This produces an AC reference. The AC reference is the compared with the load current in grid to generate reference for (PWM) inverter switching. To reduce steady state error and increase system stability (PI) type controller is used in current loop. To reduce disadvantageous perturbation of grid voltage, feed forward compensation is added to the system. This method does not change system characteristics but improves stability.

Synchronizing the PV system to the grid needs information about certain grid parameters, this information are obtained from PLL. Here synchronous reference frame (d and q axis) based control, where three phase quantity is translated into a rotating space vector, which is used to control the power flow. In this study, grid voltage vector is aligned towards d axis. So aligning of current vector to the grid d axis ensures a unity power factor operation. Separate controllers are used to control active (I_d), reactive (I_q) power, and separate voltage controller is used to control the DC bus voltage. PLL is used to track the gird frequency and voltage.

2.7.1 Phase locked loops

To supply unity power factor current and to maintain synchronism with the grid, PV system needs grid angle, voltage and frequency, Synchronous Reference Frame (SRF) PLL with moving average filters [8] implemented. Moving average filter is used to eliminate 2nd harmonic negative sequence component. Dynamics of PLL have significant role in transient behavior of PV system. Because important parameters (V_{sd},V_{sq}, sin(ρ), cos(ρ), ω) are obtained from PLL, which have significant influence in the modulation index. Figure 2.11 shows the simplified structure of SRF PLL with filter. Figure 2.12 shows the performance of PLL. In this case L-G fault is created at time t=0.25s.

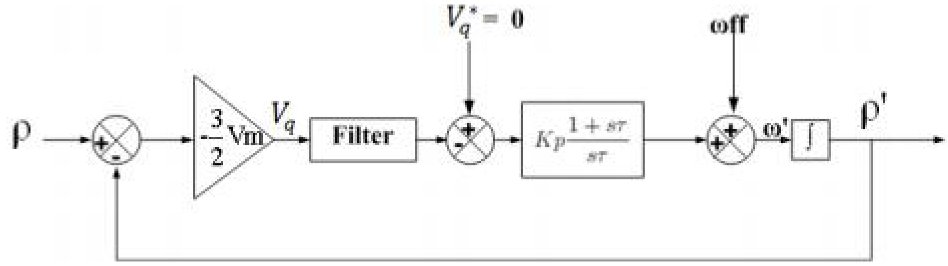

Figure 2.11: Simplified structure of SRF PLL with filter

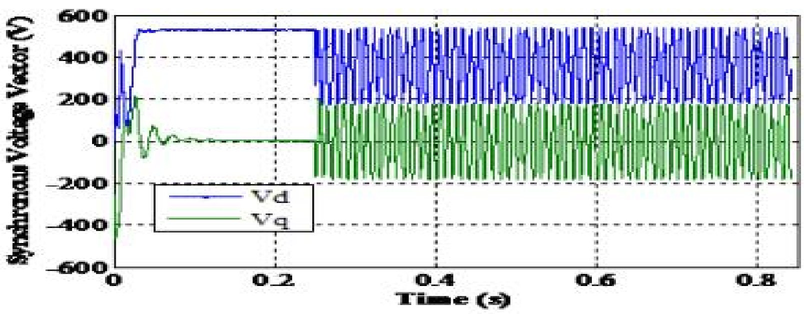

Figure 2.12: Performance of PLL during fault at t=0.25s

2.7.2 Current controller

Controls the current injected to the grid and convert the current reference I_{dref}, I_{qref} (equal to zero for Unity Power Factor (UPF)) into required inverter voltage by controlling the modulation index [9]. Figure 2.13 shows the inverter to filter to grid.

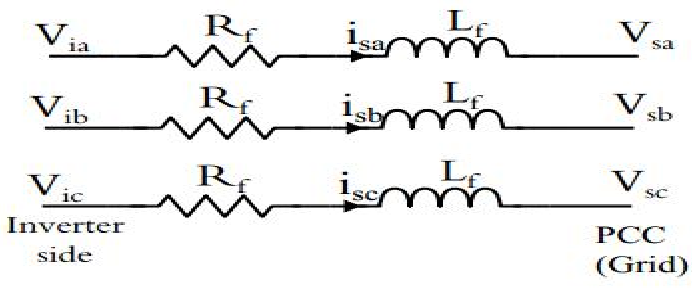

Figure 2.13: Inverter to filter to grid

Decoupled I_d & I_q are used to simplify the Multiple Input, Multiple Output (MIMO) system into two Single Input, Single Output (SISO) system From the Figure 2.13 as shown in the following equations:

$$v_{ia} = L_f \frac{di_{sa}}{dt} + i_{sa}R_f + v_{sa}$$

$$v_{ib} = L_f \frac{di_{sb}}{dt} + i_{sb}R_f + v_{sb}$$

$$v_{ic} = L_f \frac{di_{sc}}{dt} + i_{sc}R_f + v_{sc}$$

$$\text{if } v_{sa} = v_{sm} \sin \omega t$$

$$\text{for UPF } i_{sa} = I_{sm} \sin \omega t$$

$$\text{so } v_{ia} = L_f \omega I_{sm} \cos \omega t + V_{sm} \sin \omega t \quad (2.12)$$

Where v_{ia}, vi_b and v_{ic}=three phase output voltage of the inverter, v_{sa},v_{sb} and v_{sc}= three phase grid voltage, V_{sm} and I_{sm}=modulating voltage and current, ω= Grid frequency in rad/s and L_f=filter inductace. Current injected to the grid (at PCC) I_{sa} can be controlled by controlling the inverter voltage v_{ia} as given in the equation (2.12). Inverter voltage can be controlled by switching the inverter in a different modulating signal. Figure 2.14 shows the current controller block diagram.

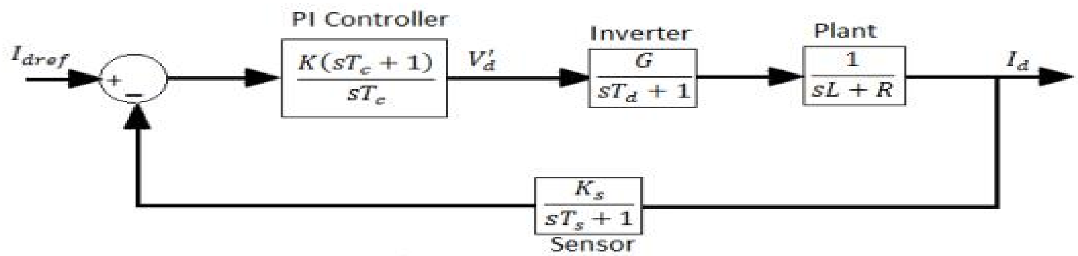

Figure 2.14: Current controller block diagram

2.7.3 DC bus capacitor voltage controller

PV is directly connected across DC bus capacitor, so voltage across capacitor must be maintain constant to harvest maximum power from the PV, also to reduce output ripple and to ensure balanced inverter output. Voltage is controlled by controlling the output current as given:

$$I_{cap} = I_{pv} - S^a I_{sa} + S^b I_{sb} + S^c I_{sc} \quad (2.13)$$

From the above equation, by controlling the current injected to the gird, DC bus capacitor voltage can be controlled. PI voltage controller is used to regulate the DC bus voltage. This controller converts voltage error to current required by the capacitor voltage PI controller gives d-axis current $I_{d\ cap}$, which must be injected to the capacitor (to regulate the voltage at the MPP level). This current is given as input to the current controller and converted into I_{dc} (actual current through capacitor) and given to the plant as in Equation (2.14). Figure 2.15 shows the voltage controller block diagram.

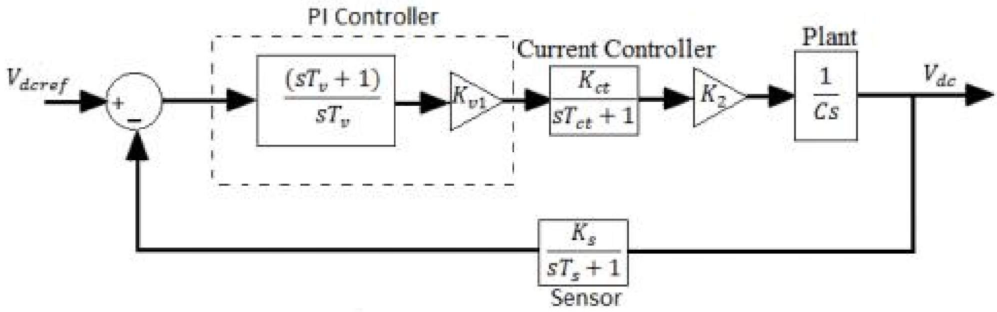

Figure 2.15: Voltage controller block diagram

$$I_{dc} = K_2 \times I_{dcap} = \sqrt{\frac{2}{3}}\frac{V_{rms}L_L}{V_{dc}} \qquad (2.14)$$

Working of the PV system model is given below:

• PV panel supplies the current (I_{pv}) based on the DC bus capacitor voltage (V_{dc}=V_{pv}).

• MPPT senses I_{pv} and V_{pv} , and set the voltage reference for the voltage controller. MPPT always perturbate the DC bus voltage towards maximum power point.

• Based on the power generated by the PV panel, synchronous current reference (I_d pv) is generated and fed to the current controller to inject all possible PV power to the grid.

• Voltage controller try to regulate the DC bus voltage as dictated by the MPPT and generate the capacitor synchronous current reference (must be injected to the capacitor) to regulate the voltage. It fails during power imbalance (e.g. fault).

• Capacitor current reference is subtracted ($I_{d\ pv}$− $I_{d\ cap}$) from the PV current reference and given to the current controller as the reference current ($I_{d\ ref}$).

• Current controller sets the inverter pole voltages based on the current reference and control the power flow to the grid, for maintaining UPF I_{sq}=0.

• Based on the grid voltage (at PCC) space vector magnitude (V_{sd} and V_{sq}) with its angle (ρ), current controller sets the inverter voltage space vector (V_{id} and V_{iq}) with certain angle to control the current. So based on the grid voltage, PV system supplies the current.

• PLL is used to track the grid voltage space vector and its angle, this is given as an input to the current controllers, so all transformation is carried out based on the grid space vector angle.

• Forcing current space vector lie on the gird voltage vector assures UPF operation. PLL gives voltage, phase and frequency information of the grid. So it is act as an important role in synchronization.

• Frame transformation is used to convert all the synchronous quantity to a actual three phase quantity (d-q to a-b-c). by using inverter pole voltages (set by the current controller) and the grid voltages, PV output currents are computed and injected to the grid at PCC.

• PV system injects current to the grid based on the available PV power and grid voltage.

2.8 General Protection Issues in Distributed Generation

This section describes the various issues associated with system protection in Distributed Generation (DG).

2.8.1 Protection coordination issues

There are several new situations introduced when there is a possibility of bidirectional power flow. These situations were not considered when designing the protection systems of present distribution networks which are based on radial power flow. These issues were studied by Brahma and Girgis [10] and are discussed in this section. In Figure 2.16, if we consider that no distributed generator (DG1) is connected, for a coordinated system, fuse F1 and fuse F2 are selected so that for any fault on feeder1, F1 operates before

F2. This is possible if Total Clearing (TC) characteristic of F1 is below the Minimum Melting (MM) characteristics of F2 by a safe margin for any feeder fault.

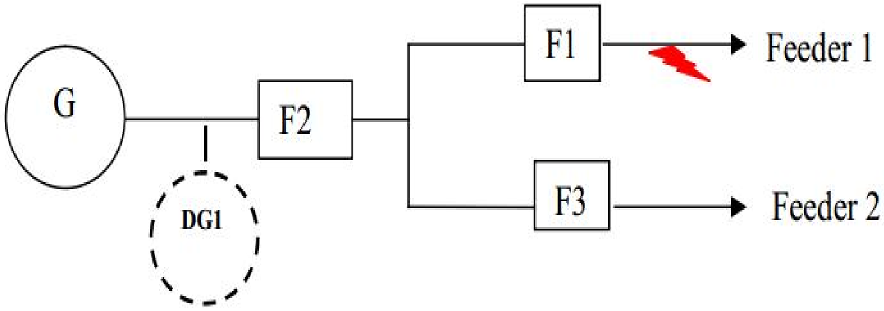

Figure 2.16: DG1 connected upstream of fault location

For the same network, if a distributed generator DG1 is added as shown in Figure 2.16 and consider a fault in feeder1, the maximum and minimum fault current will increase from the source side due to the upstream DG unit. In this case fuse coordination is not likely to be affected if fuses can still coordinate with the changed level of fault currents. This is because fuses will see only downstream faults. For the same network, if a distributed generator DG2 is connected in the downstream of feeder 1, for a fault as shown in Figure 2.17, fuse F2 has to operate before fuse F1 to maintain system reliability. This is not achievable as both F1 and F2 will see same magnitude of fault current in either case (i.e. for both downstream and upstream faults). This illustrates a case of fuse-fuse coordination problem with distributed generator in network.

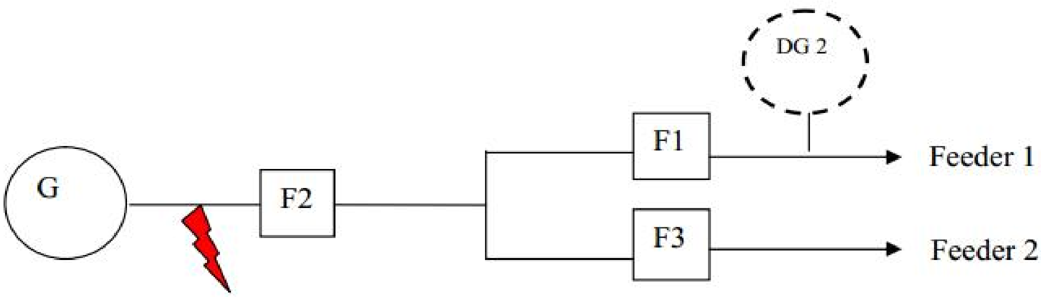

Figure 2.17: DG1 connected downstream of fault

In the network discussed above a distributed generator DG3 is added as shown in Figure 2.18 and two different cases of faults are considered and the impact of DG size on protection coordination.

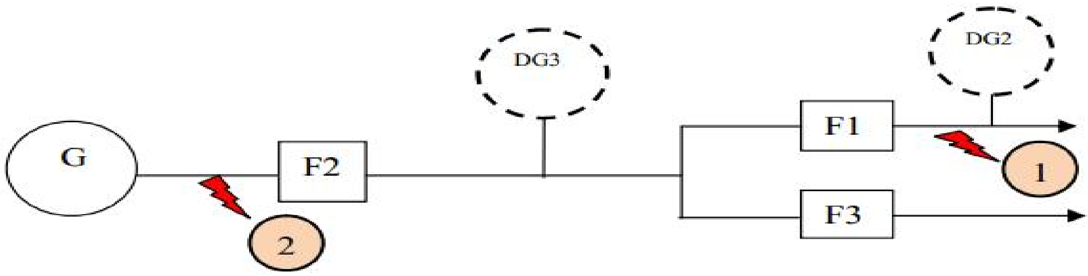

Figure 2.18: Impact of DG size on fuse coordination

If fault occurs at location 1, current passing though fuse F2 (IF2) is less than the current flowing through fuse F1 (IF1), while if fault is at location 2, IF2 is greater than IF1. The difference in magnitude of IF1 and IF2 depends on the size of generator DG3. When (IF1>IF2) the coordination always holds well. When (IF2>IF1) the difference between the magnitude of IF1 and IF2 decides the level up to which the coordination will hold well. If the difference in magnitude between IF1and IF2 is not above a minimum value, the coordination will not hold well. As the difference in the magnitude of IF2 and IF1 depends on the size of DG3, when the size of DG3 exceeds a size which is adequate to provide enough fault current to ensure minimum difference in magnitude between IF1 and IF2, the protection coordination will not be disturbed. Distributed generator also has the potential of disturbing the protection coordination between fuse and recloser. This issue has been discussed in details in several papers [10-13]. The recloser fuse coordination problem caused by distributed generators has been described below. In the network shown in Figure 2.19, it is initially assumed that the DG is not connected.

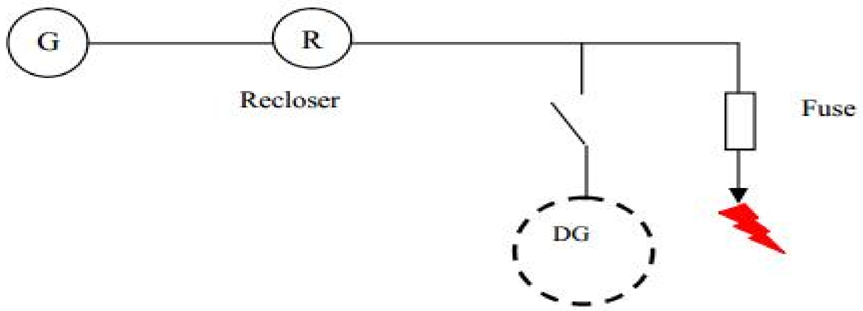

Figure 2.19: Fuse – recloser coordination –impact of DG placed between recloser and fuse

2.8.2 Impact of fault current limiters in distributed generators

To minimize the impact of DG in Power Delivery Systems (PDS) an alternate approach was studied by El Khattam and Sidhu [14]. The concept is to introduce Fault Current Limiters (FCL) to limit the impact of DGs during fault. The current practice is to disconnect DGs during fault to restore original relay coordination. This however, causes loss of DG power due to temporary faults and synchronization problems for reconnecting those DGs into PDS. By using FCL in series with DGs to limit fault current helps in suppressing the DG impact on original relay setting during faults. If this approach is used disconnection of DG during faults is not required.

In this approach most optimal relay setting are obtained by minimizing the total primary operating time in the original PDS without DG in two phase process. In the two phases proposed optimization model, phase I model is formulated as nonlinear programming and phase II model is formulated using linear programming. When DG is introduced in the system the original coordination of PDS will be disturbed. Based on the optimum relay settings and engineer's experience, the FCL impedance, type and minimum value, required to restore the original PDS relay coordination are provided with Revised Coordination Time Interval (RCTI) between relays. The relay setting optimization method is described in the section below. The total time objective function J for N primary relay near end fault is minimized, subject to various constraints. These constraints are relay setting constraints and back-up relay constraints.

Minimize $j = \sum_{i=1}^{n} t_i$ (2.15)

2.8.3 Fault contribution of distributed generators

As discussed earlier, fault current contribution from the distributed generator disturbs the existing relay coordination system designed for radial distribution systems. While the fault current will always be increased by adding generation, the consequences on the fault clearing elements can be in two opposite directions. If a fault occurs upstream of fault clearing device (i.e. towards substation), the clearing device will see the current flowing upstream to contribute to the fault. If a fault occurs downstream of the fault detection and clearing device , the fault seen by the clearing device will be reduced and may even be shadowed by the contribution of local generation and thus remain undetected.

Turcotte and Katiraei [15] discussed the issues of DG interconnection in terms of total fault current contribution and changes in short circuit capacity requirements of circuit breakers or under load disconnecting switch only. The circuit breaker must carry fault current until opening of protective device. The minimum opening time of circuit breaker is 3, 5 or 8 cycles. Consequently a DG source capable of tripping within 50 ms will have no effective contribution to short circuit capacity of system. The investigation highlights the distinction between rotating machines and inverter based power sources with respect of their fault contribution.

2.8.4 Impact of PV inverters on system fault levels

PV inverters are Inverter Interfaced Distributed Generators (IIDG) and the fault current contribution varies considerably due to fast response of inverter controller. In a conventional distribution system, substation is the only source of power, and since substations are generally away from generating units, the fault current transients usually do not have the initial high sub-transient component. Therefore the fault current is usually approximated by its steady state value and the feeder can be represented using a steady state model where the substation can be represented by a Thevenin's equivalent and the lines can be represented by series impedances. The corresponding circuits can be analyzed using nodal equations.

$$Y_f \times V_f = I_{in\ j} \qquad (2.16)$$

Where Y_f is the node admittance matrix, V_f is the voltage at each node and I_{inj} is the current injected at each node. If there are conventional synchronous generators on feeder then the above feeder model can be extended easily by simple Thevenin's equivalent model of generators. However, for IIDG the same technique cannot be applied. This issue has been discussed by Baran and Markaby [16] and the new approach required in order to incorporate IIDG into fault analysis is described in the subsequent paragraphs. Figure 2.20 shows the block diagram of inverter interfaced DG.

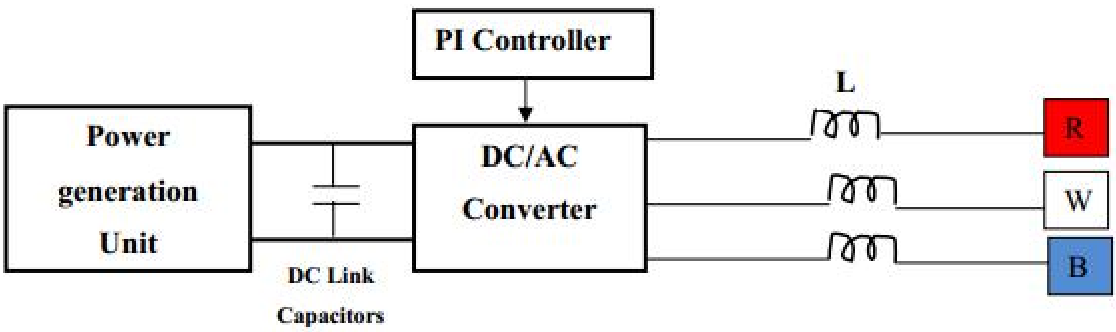

Figure 2.20: Block diagram –inverter interfaced DG

During a transient the IIDG response mainly depends mainly on the inverter controller. There are two main control schemes for inverter controller:

- Voltage based scheme – Converter helps inverter to synthesize a three phase balanced ac voltage at the inverter terminals. To regulate the real and reactive power output of DG the controller adjusts the amplitude and phase of the synthesized inverter voltage with respect to terminal voltage.

- Current control scheme –This scheme uses two loops, the inner loop controls the power output of DG and outer loop regulates the power output. The outer power controller acts like a supervisory controller and determines (I_{ref}) for the fast inner current controller.

CHAPTER THREE
MATHMATICAL MODEL

3.1 Background

PV system with distributed network is simulated in MATLAB/SIMULINK environment, since the model have many subsystem and dynamic elements, and simulation takes much time to simulate the system.

• Distribution voltage at PCC (bus 1) takes much time to reach steady state, because during initial time, distribution system act as a voltage source connected to an R-L-C circuit.

• Due to oscillation in the distribution system, PV system, which sense the PCC voltage takes much time to reach steady state

• PLL have to reach the steady state before PV system starts its operation, since MATLAB try to execute all the blocks simultaneously, so PV system oscillates for long time.

• MPPT must start with the better voltage otherwise, due to MPPT dynamics, system will take much time to track the maximum power point.

• Less DC bus capacitor initial voltage results in an oscillations in the current and voltage controller, this leads to an injection of high current to the system and slower the process of reaching steady state.

• Both voltage and current controllers have saturation blocks to limit the maximum current (rate of change in the current), since during initial condition many system parameters are oscillating, limitation of the controller results in, inability of the controller to speed up the settling process.

• Since switching frequency set to 5KHz and sampling time to 0.1ms, fixed point MATLAB simulation time must kept very low to record the dynamics, this leads to very high simulation time, most often computer/hardware failed to simulate the model.

• Power balance added in the voltage loop leads to an initial DC bus voltage oscillation, any change in the DC bus voltage leads to the change in the present MPPT voltage; this makes system to stabilize at slower rate, since MPPT is relatively slower than the other dynamic elements in the system.

There is a need to reduce the initial settling time of the system, because many disturbances must be simulated, while system is in the stable condition. Methods employed to reduce settling time of the system must not affect the performance (dynamics) of the system [5].

3.2 Simulation Requirement

Simulation method must satisfy the below requirement:

• Simulation must take less time.

• It must be scalable to any distribution network.

• User friendly.

• Must adopt standard input format.

Here system is divided into two parts:

• Non linear PV system.

• Linear distribution system distribution line load.

3.3 PV System Parameters

The under study case consists of two identical plants have a total capacity of 1 MW (500KW for every plant). Each plant consists of five PV array (100KW for each one) connected in parallel interfaced with distribution system.

3.3.1 PV array

Implements a PV array built of strings of PV modules connected in parallel, each string consists of modules connected in series. Allows modeling of a variety of preset PV modules available from NREL system advisor model as well as user-defined PV module. The PV array has two inputs, Input 1=Sun irradiance, in W/m^2, and input 2=Cell temperature, in deg.C. Table 3.1 shows the description of PV array which used in design.

Table 3.1: Description of PV array

Element	Description
PV array	• Parallel strings=64 • Series-connected modules per string=5 • Maximum power =315.072w/module • Module voltage at maximum power point V_{mp} (V)=54.7V

3.3.2 Inverter

Since, main focus is on studying transient response for large signal disturbances, so harmonics generated by the inverter is not of much interest. So average model of inverter is sufficient for the analysis, but simulation carried out for both systems with and without inverter shows no significant difference found. Inverter design details as following:

- Two level three phase inverter with the rating of 500KW.
- Sine triangle PWM with a switching frequency equal to 5KHz.
- LC filter is used.
- Inverter is modeled as a first order system with the time constant equal to the half of switching time (bandwidth is equal to twice that of switching frequency).
- Constant current mode control is used to inject UPF power to the grid.
- Voltage controller is used to regulate the DC bus voltage.
- The parameter of the controller had chosen using symmetrical optimum method. value of k_p = 0.5 and T=0.08.

3.4 Distribution System Parameters

Lumped parameters are used to model [17] the distribution system, simple radial 4 bus distribution system is considered. Table 3.1 shows the system given parameters as per IEEE 1547 standard.

Table 3.2: System parameters as per IEEE 1547 standard

Parameter	value
Q_f	1.7
f	50Hz
R_s/Z_s	0.15
Cs	1µF
L_f	0.1088mH
C_f	470µF
Fs	545.57Hz
C_{1f}	470µF
C_{2f}	0.0743µF
R_f	1.02mΩ
T_c	0.1057s
K	0.272
K_v	0.002s
K_s	1

3.4.1 Modeling of load

Simple RL load with a capacitor reactive power compensation is modeled; capacitor must be chosen such that resonance will happen at rated frequency (50Hz). Load equations as following:

$$R_L = \frac{V^2}{P_{load}} \quad (3.1)$$

$$L_L = \frac{V^2}{Q_f P d_{load} d\omega} \quad (3.2)$$

$C_L = \frac{Q_f Pd_{load}}{\omega V^2}$ (3.3)

$\omega = 2\pi f$ where f = 50Hz

Case study Line voltage V = 33Kv

3.4.2 Infinite grid model

Here substation is modeled as an infinite grid by using its short circuit MVA (SMVA).

SMV A = 500MW

V = 33kV

for $\frac{R_s}{Z_s} = 0.15$

$Z_s = \frac{V^2}{SMVA} = 2.178\Omega$

(3.4)

$R_s = 0.15\times Z_s = 0.3267\Omega$

$L_s = \frac{\sqrt{{Z_s}^2 - {R_s}^2}}{\omega} = 6.86\ mH$ (3.5)

3.4.3 Transformer

Transformer (Δ−Y) is modeled by using its leakage reactance and the resistance, all parameters are translated with respect to high voltage secondary. Leakage reactance are calculated using its short circuit test voltage (V_{sc}), inverter grade transformer is designed for relatively high leakage reactance, so V_{sc} = 8%.

P_{rated} = 1.25MW

%V_{sc} = 8%

Efficiency η = 99.8%

HV side current $I_{rated} = \frac{P_{rated}}{V_{rated}} = 21.87$ (3.6)

Voltage drop $V_L = \frac{\%V_{sc}V_{rated}}{\sqrt{3}}$

$R = \frac{(1-\eta)P_{rated}}{3{I_{rated}}^2} = 1.74\ \Omega$ (3.7)

$L = \frac{V_L}{\omega} = 0.222\ H$ (3.8)

So Transformer $\frac{X}{R} = 40$

3.4.4 Distribution line model

The system under consideration has three distribution lines, conductor area of the transmission line is chosen based on short circuit MVA and its continuous current carrying capability. Resistivity (ρ) of the line is considered as 1.25 times of the given copper resistivity (at20^{o} C).

X_t = 0.4Ω/km (for 33kV Line)

$$L = \frac{X_t l}{\omega} \qquad (3.9)$$

$$R = \frac{1.25\rho l}{A_c} \qquad (3.10)$$

Table 3.3 shows the lines Parameters.

Table 3.3: Lines parameters

Line No	Length(km)	Inductance $L(mH)$	Resistance (Ω)
Line 1	4	5.1	1.2
Line 2	5	6.4	1.6
Line 3	7	8.9	4.9

All above equation modeled using MATLAB SIMULINK as shown in appendix (A). Overall program model involves modeling of full PV system (includes modeling of photovoltaic panel, controllers, MPPT, PLL), manufacturer data sheet based PV panel is modeled. Constant current control based UPF interface is used to connect the PV system to the grid. Distribution system which assumes infinite grid as a source was modeled. The overall PV system is modeled such that it takes very less time for simulation. The given system is implemented by using MATLAB/SIMULINK. System model also takes care of unbalanced conditions. This model can be used for any number of distribution system, system model is used to simulate the different disturbances, effect of each PV system element for different disturbances.

CHAPTER FOUR

RESULTS AND DISCUSSION

4.1 Introduction

PV system model is simulated for different grid disturbances and effect of each PV system dynamic element on a particular disturbances are analyzed. Important dynamic elements in the PV systems are MPPT, voltage controller (with DC bus capacitor),PLL and current controller (with filter inductor). The system studied under different conditions.

4.2 Normal Operation of Full PV System

PV System is operated at the irradiance of $1000W/m^2$ and $T_{cell}= 25^o$, frequency of 50Hz and grid voltage of 1pu at PCC. Figure 4.1 shows the PV system response at normal conditions, performance of the PV system model found satisfactory and matches with the actual data.

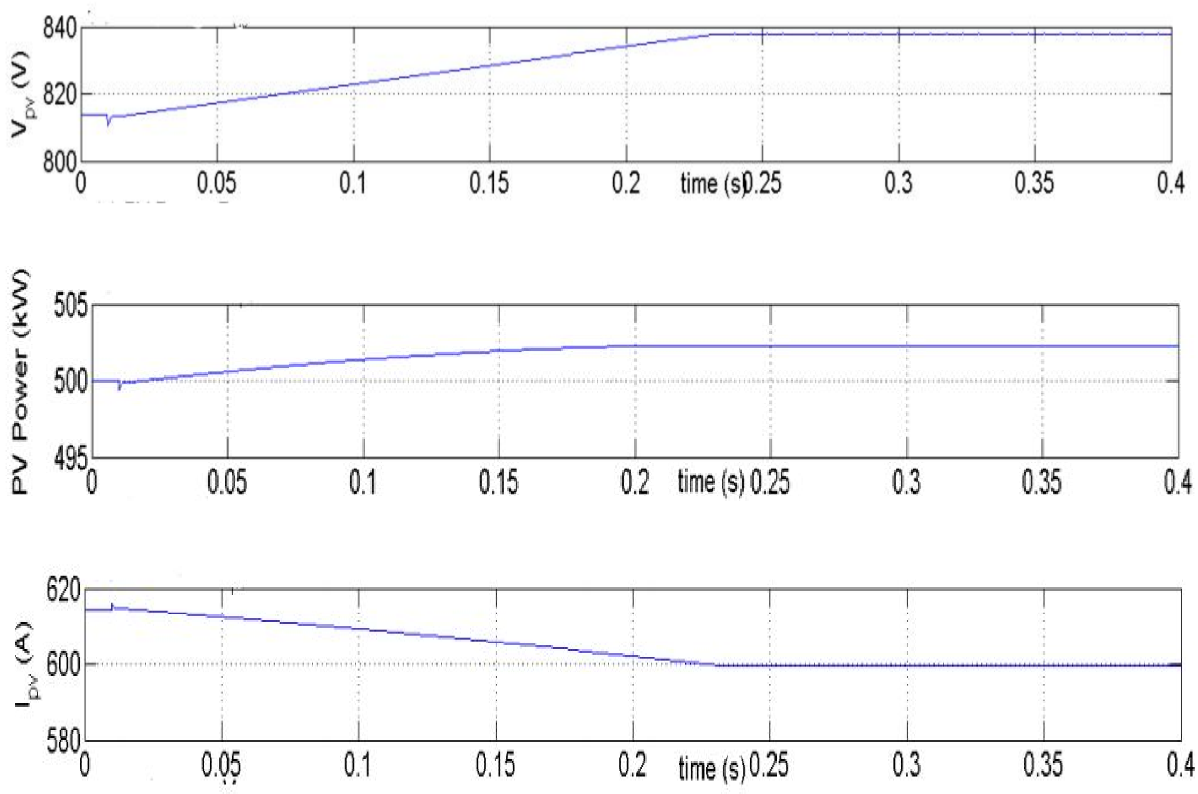

Figure 4.1: PV system response at normal condition

4.3 Change in Irradiance from 1000W/m^2 to 500W/m^2

Irradiance E is changed from 1000W/m^2 to 500W/m^2 at time t=0.25s. Since MPPT is the important dynamic element for environmental change. Simulation is done for two different MPPT perturbation (0.1 and 0.01). Study is carried out on PV system with the capacity of 500KW. Figures 4.2 and 4.3 shown the Change in irradiance and PV three phase current injected to the grid.

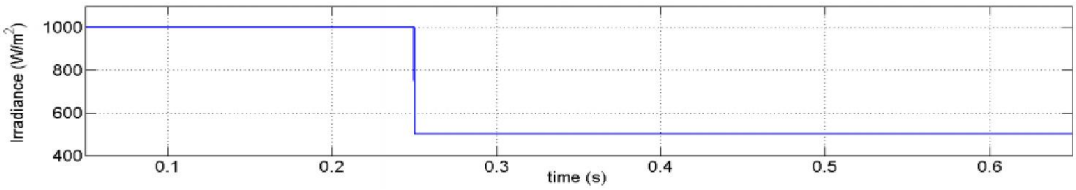

Figure 4.2: Change in irradiance

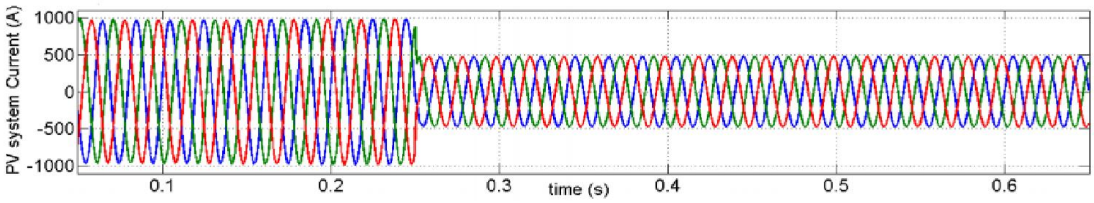

Figure 4.3: PV three phase current injected to the grid

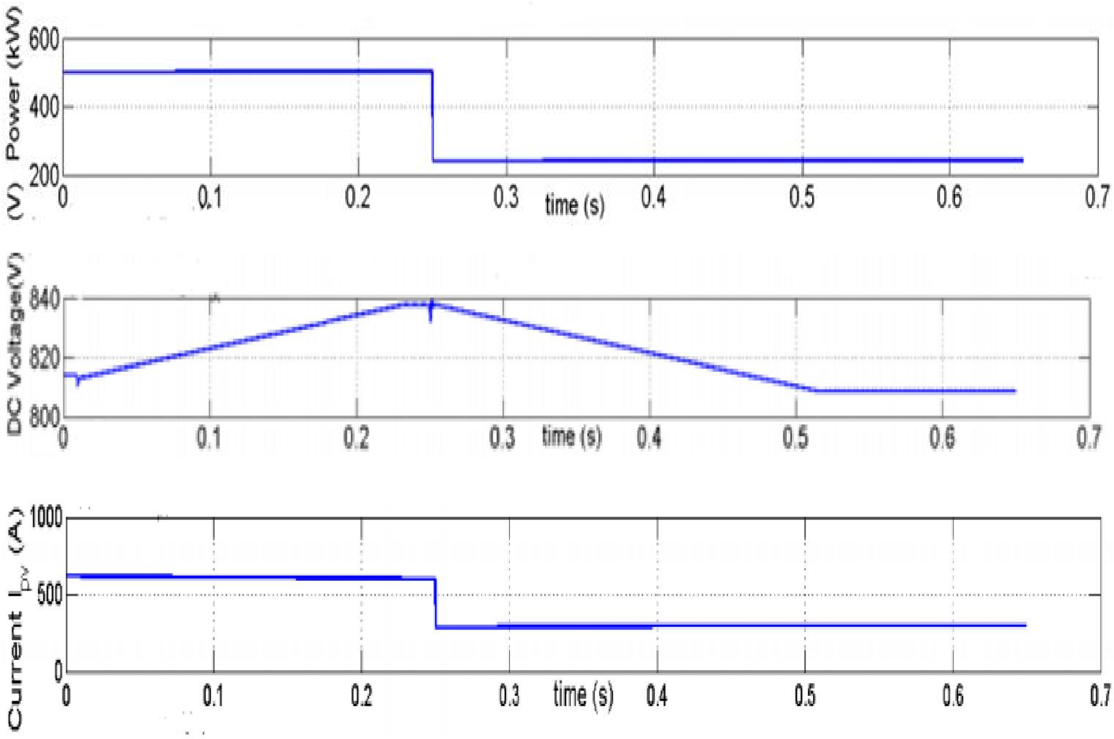

Figure 4.4: PV system response for irradiance change (1000W/m^2 to 500W/m^2) MPPT=0.1

From Figure 4.2 and Figure 4.3 the total three phase current injected to the grid decreased from 1000A to 500A due to sudden change in irradiance from1000W/m^2 to 500W/m^2 at time t=0.25s. Effect of this disturbance in the grid is very less, since grid is stronger and local load also less than PV system, so no significant change found in grid voltages. Figure 4.4 shows the System response with action of PLL. From Figure 4.4 concluding remarks are

- Slight dip in the capacitor voltage due to the pre disturbance (t=0.25s).
- The current decreased to the half, so the power also reduced.
- PLL doesn't have any effect on dynamics of the PV system during climatic disturbances.

Figure 4.5 shows the system response with action of (V and I) controllers.

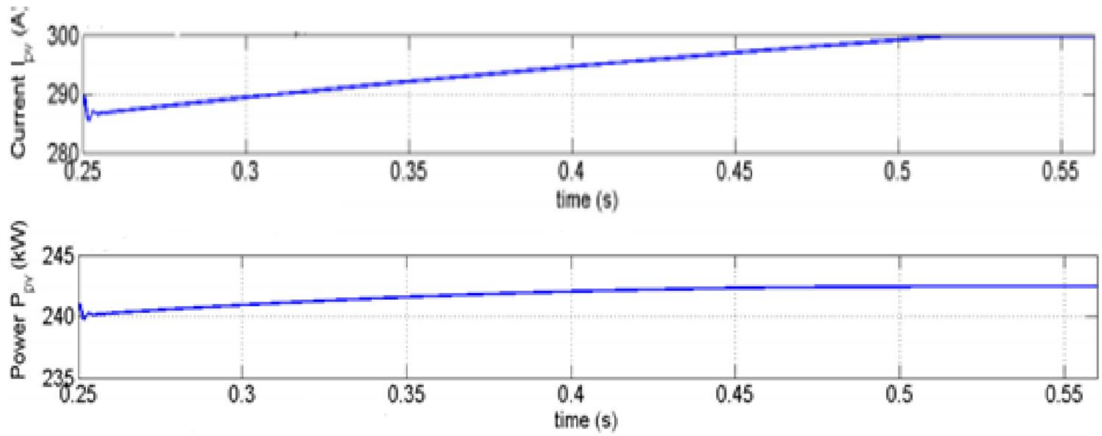

Figure 4.5: Portion of PV current and power after insertion of (V and I) controllers at MPPT=0.1for change in irradiance

To study the effect of MPPT, perturbation is changed from 0.1 to 0.01, system response as shown in Figure 4.6.

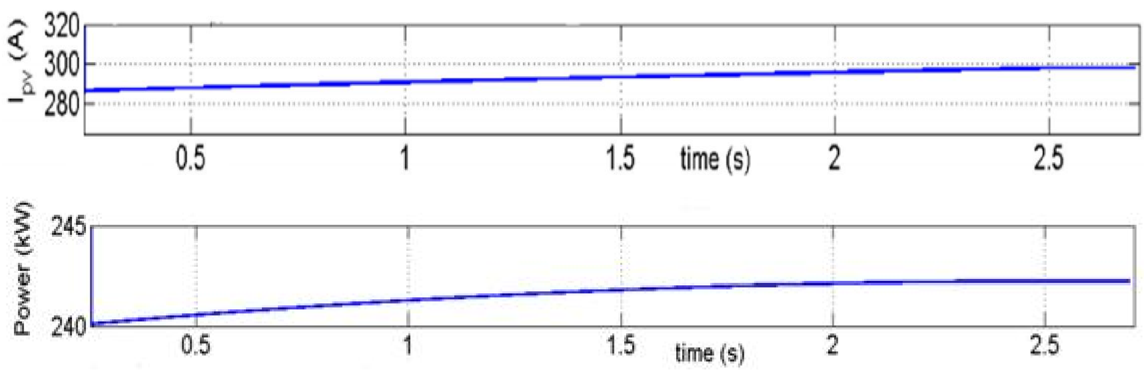

Figure 4.6: Portion of PV power after insertion of (V and I) controllers at MPPT=0.01for change in irradiance

Figure 4.5 shows the system response with current and voltage controllers.

From Figure 4.5 concluding remarks are:

- The bandwidth of the current control loop is around 2500 rad/s, and voltage controller is around 1100 rad/s. so system will need minimum of 0.4ms to settle.
- System response improved, current increased due to the action of voltage controller which dictated by MPPT.

From Figure 4.6 concluding remarks are:

- System response need more time to stabilize (2.5s) when compared with previous case at figure 4.5 which took (0.5s) to settle.
- MPPT act an important role in system dynamics due to change in irradiance.

4.4 Grid Voltage Disturbance

Response of photovoltaic plant for variation in the grid voltages at PCC is analyzed by using MPPT perturbation=0.1.

4.4.1 Grid voltage variation from 1pu to 0.85pu at t=0.25s

Simulation is done for irradiance =1000W/m^2 and T_{cell} = 25^{o}c. Figures 4.7 and 4.8 shows the grid three phase voltage at PCC during voltage disturbance and PV output three phase current during voltage disturbance.

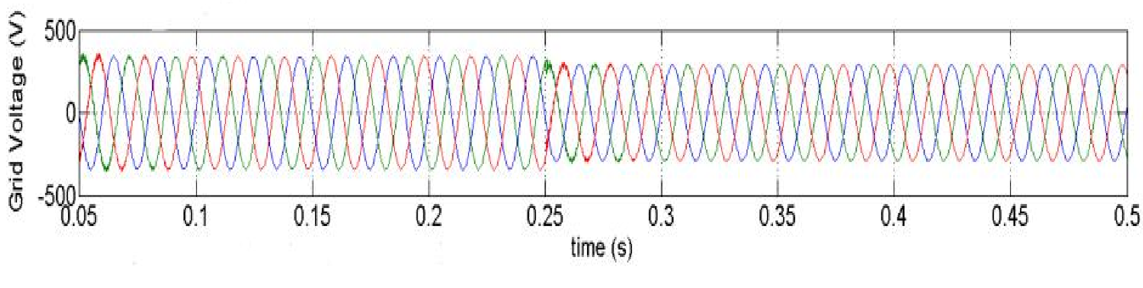

Figure 4.7: Grid three phase voltage at PCC during voltage disturbance

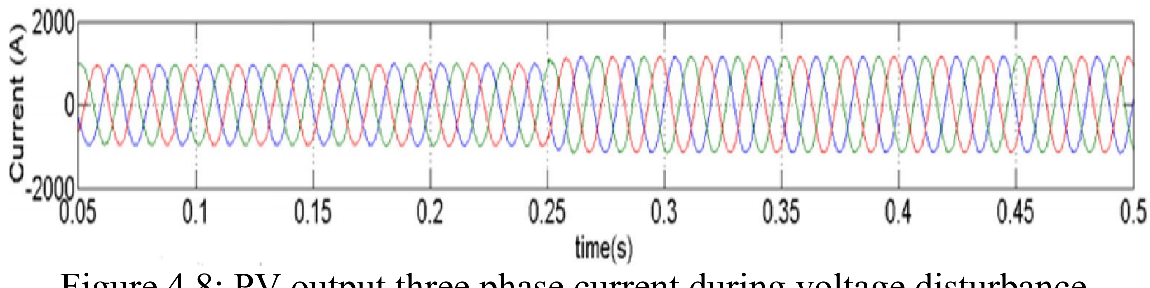

Figure 4.8: PV output three phase current during voltage disturbance

As shown in figure 4.8 the output current increased at (t=0.25s) due to the decreasing of grid voltage from 1pu to 0.85pu. Figure 4.9 shows the PV power, current, voltage and PLL voltage during voltage disturbance with action of PLL.

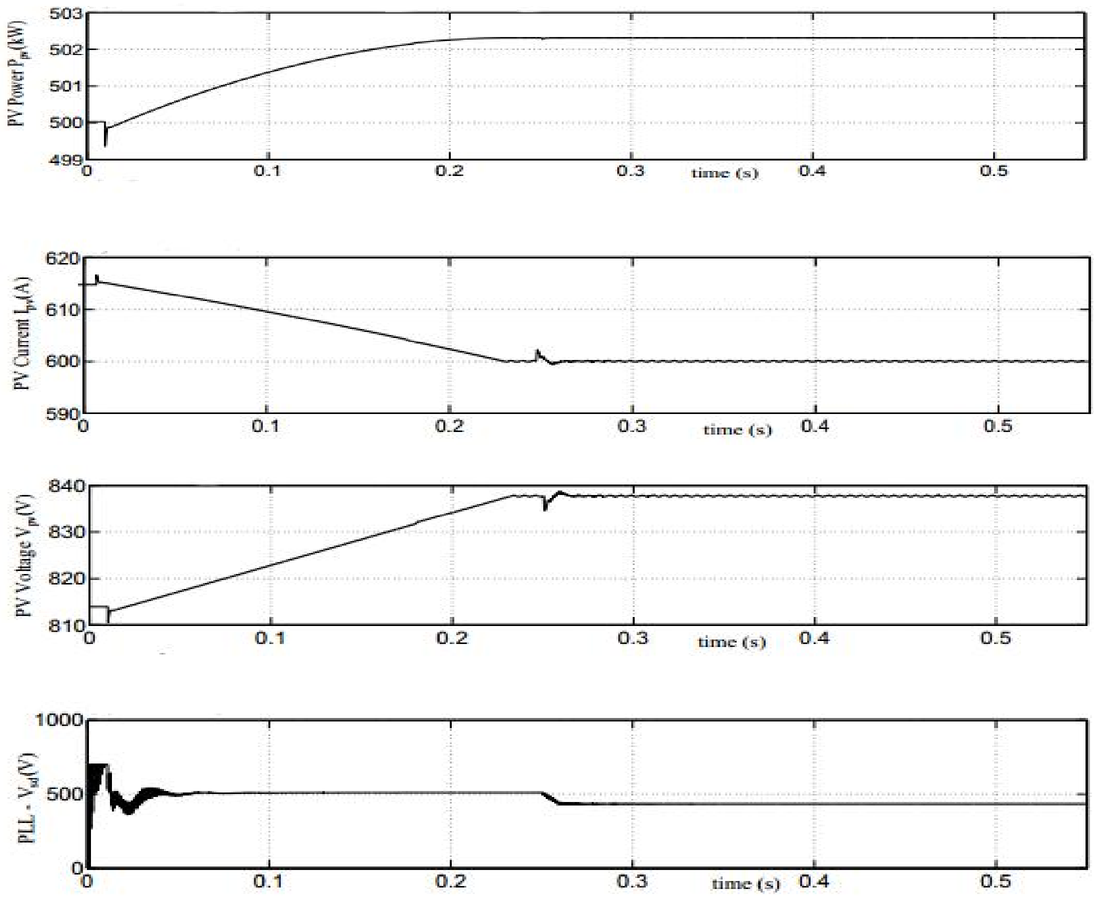

Figure 4.9: PV power, current, voltage and PLL voltage during voltage disturbance

From Figure 4.9 concluding remarks are:

- Slight dip in current and voltage due to the pre disturbance (t=0.25s).
- The no significant change found in system response (current, voltage and power).
- PLL acts as an important role in system dynamics, since PLL is the element which informs the PV system about the grid voltage vector. Based on the voltage vector PV injects power to the grid. So PLL act as an important role in PV system dynamics for grid voltage variation.

Figure 4.10 shows the system response with action of current and voltage controllers.

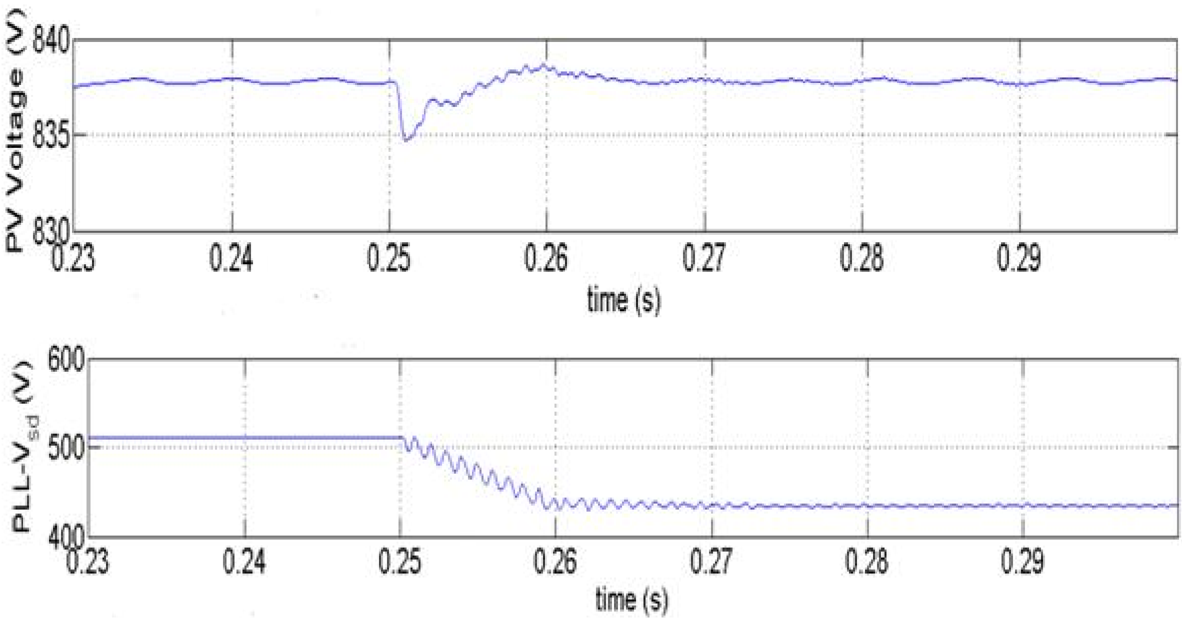

Figure 4.10: Transient portion of PV voltage and PLL voltage with (V and I) controllers during voltage disturbance

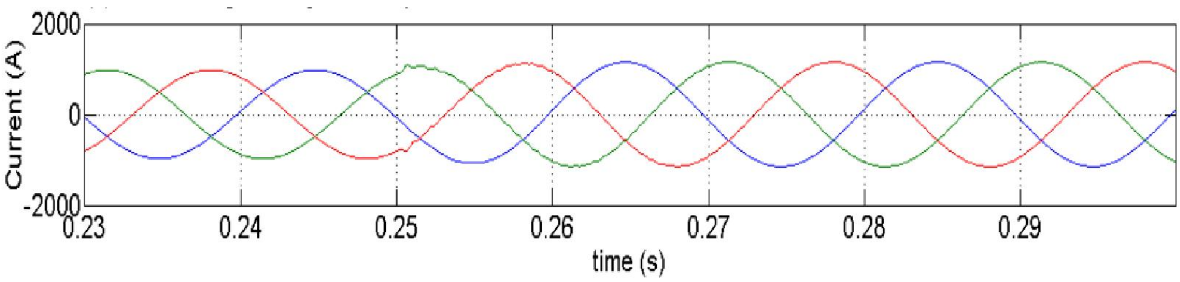

Figure 4.11: PV output three phase current with (V and I) controllers during voltage disturbance

From Figure 4.10 and Figure 4.11 concluding remarks are:

- DC bus capacitor compensated the voltage but there is small distortion on voltage wave due to voltage disturbance at (t=0.25s) as shown in Figure 4.10.
- There is no significant change in grid current although the grid voltage decreased from 1pu to 0.8pu due to action of current controller.
- Voltage and current controller have influence in the dynamics.

To study the effect of MPPT in this case, perturbation is changed from 0.1 to 0.01as shown in Figures 4.12 and 4.13.

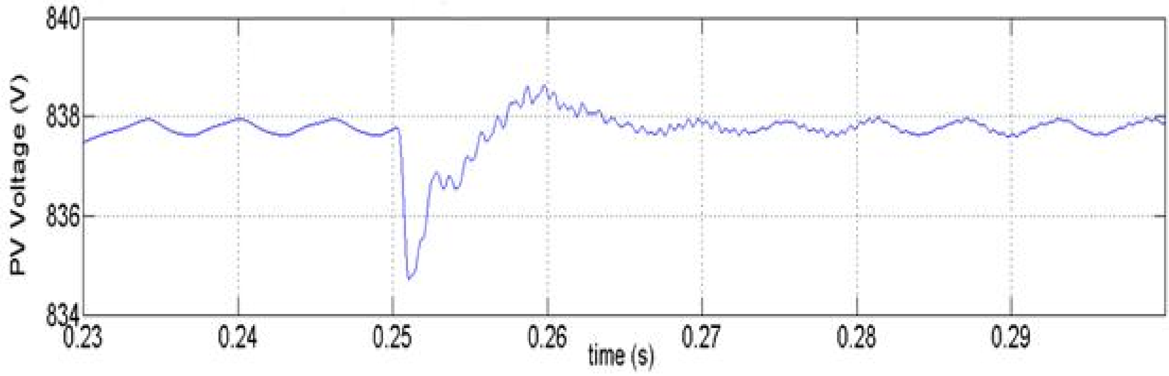

Figure 4.12: Transient Portion of PV voltage at MPPT=0.1 during voltage disturbance

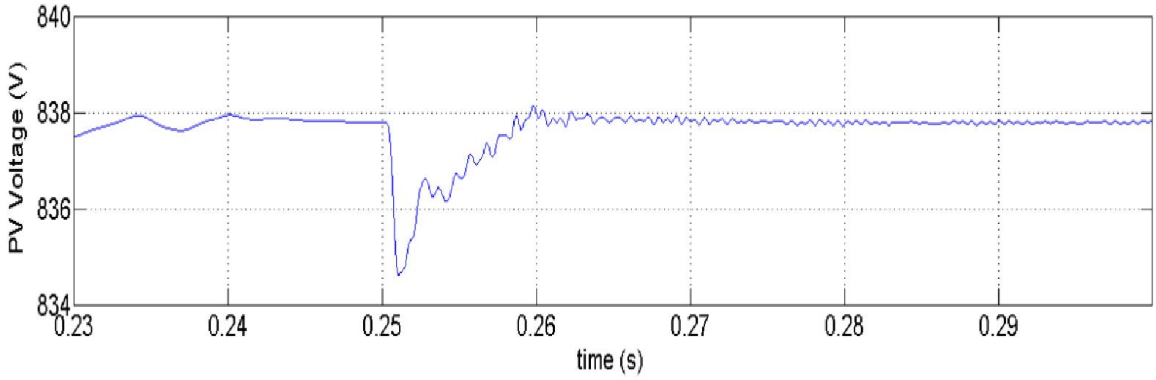

Figure 4.13: Transient portion of PV voltage at MPPT=0.01 during voltage disturbance

Concluding remark:

- MPPT has very less influence on the grid voltage disturbances. This is only true when voltage controller is employed to control the DC bus voltage.

4.4.2 Grid voltage variation from 1pu to 1.1pu at t=0.25s

Simulation is done for irradiance=800W/m^2 and T_{cell}= 25^{o}c. Figure 4.14 shows the transient response of the PV system for grid voltage variation 1pu to 1.1pu in grid voltage.

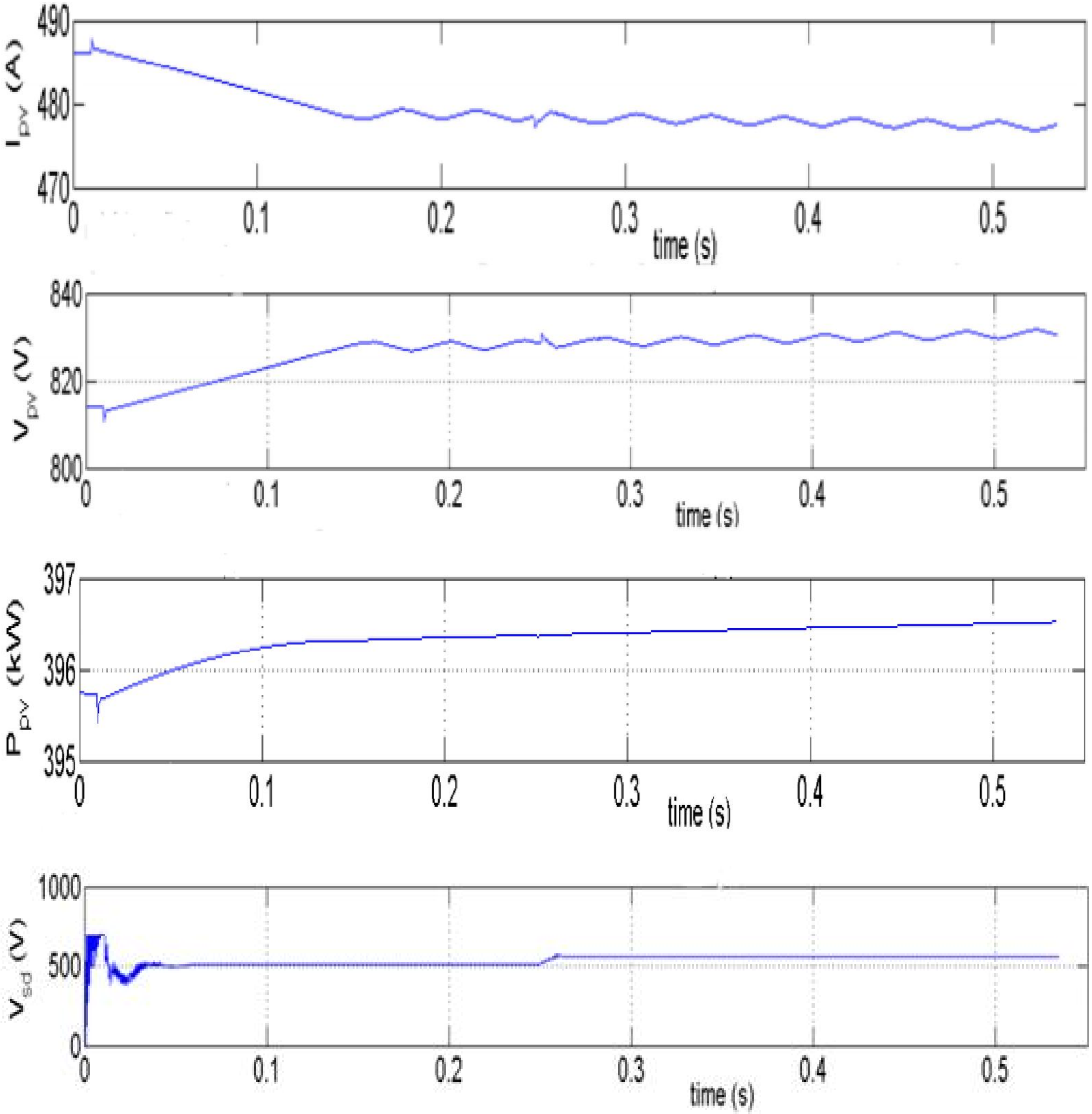

Figure 4.14: Transient response of the PV system for grid voltage variation 1pu to 1.1pu in grid voltage

Remarks are as same like previous one.

4.5 Change in Grid Frequency

Change in grid frequency from 50 to 45Hz at time t=0.25s is simulated under climatic conditions E=1000W/m^2 and T_{cell} = 25^{o}c. Figure 4.15 shows the PLL dynamics for grid frequency variation from 50Hz to 45Hz.

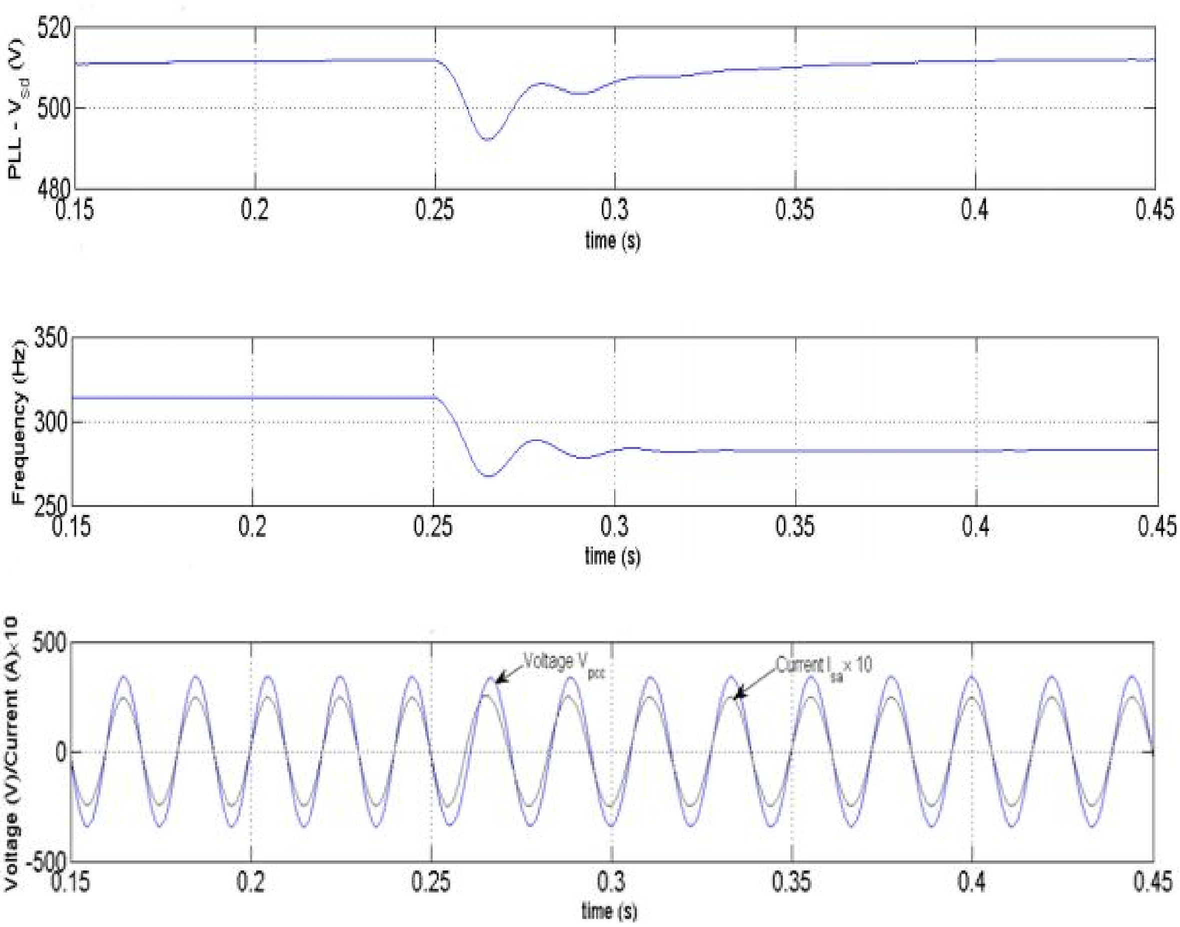

Figure 4.15: PLL dynamics for grid frequency variation from 50Hz to 45Hz

Concluding remarks:

• It observed that only PLL and current controllers have considerable effect on dynamics behavior of the system. PV system able to track frequency within a half cycle.

• MPPT & voltage controller will have very less impact.

4.6 Three Phase Fault

Three phase fault is created on the transformer high voltage secondary terminal, under the climatic condition of E = 1000W/m2 and T_{cell} = 25^{o}c at t=.025s. Simulation is carried out for different controllers and MPPT perturbation. Figure 4.16 shows the single line schematic of distribution system.

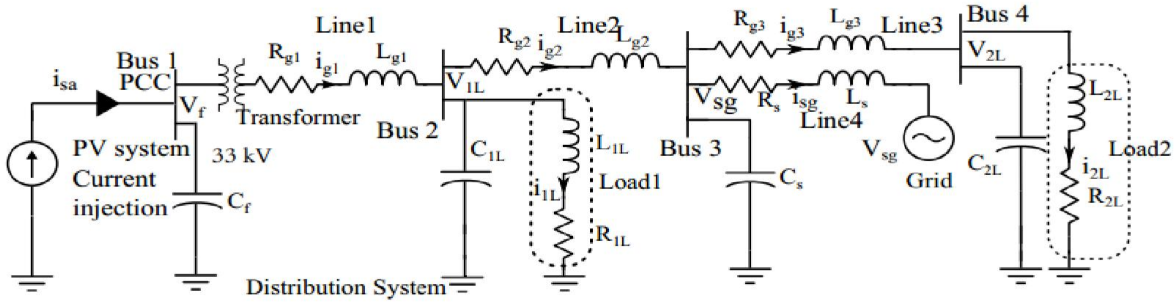

Figure 4.16: Single line schematic of distribution system

Figure 4.17 shows the grid voltage and current during fault.

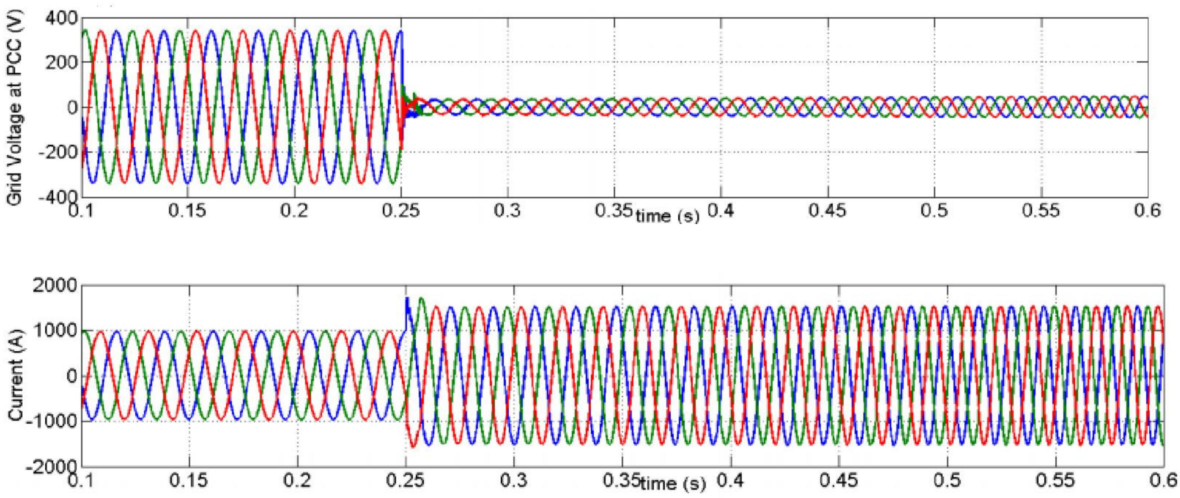

Figure 4.17: Grid voltage and current during fault

Figure 4.18 shows the system response with action of PLL.

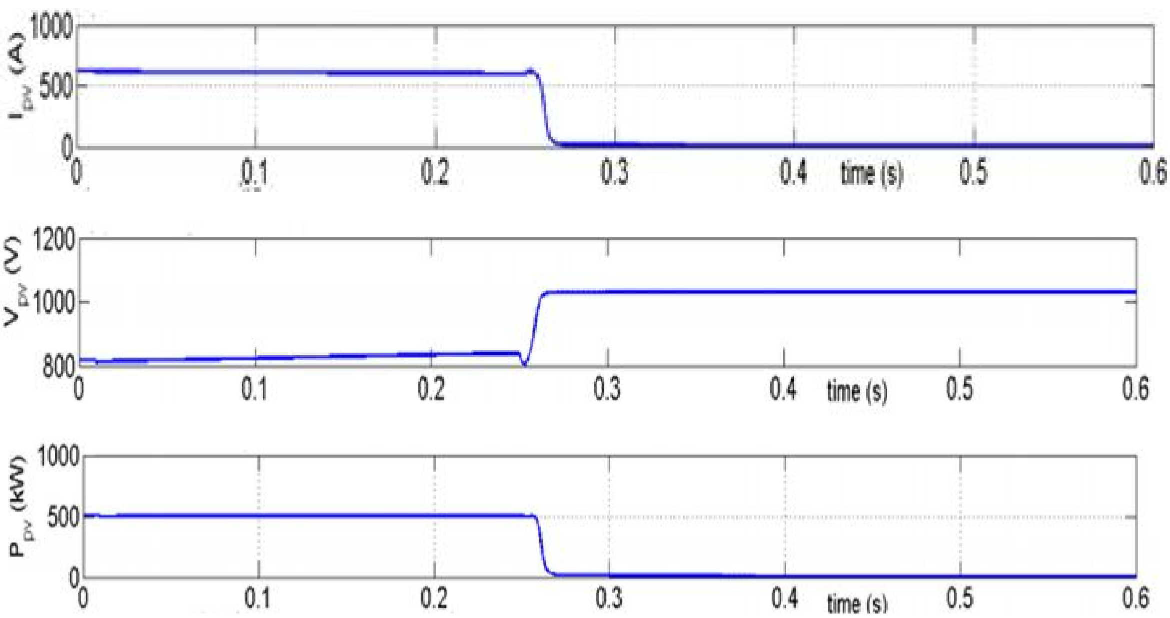

Figure 4.18: Transient response of the PV system during three phase fault with PLL

Figure 4.19 shows the system response with action of (V and I) controllers.

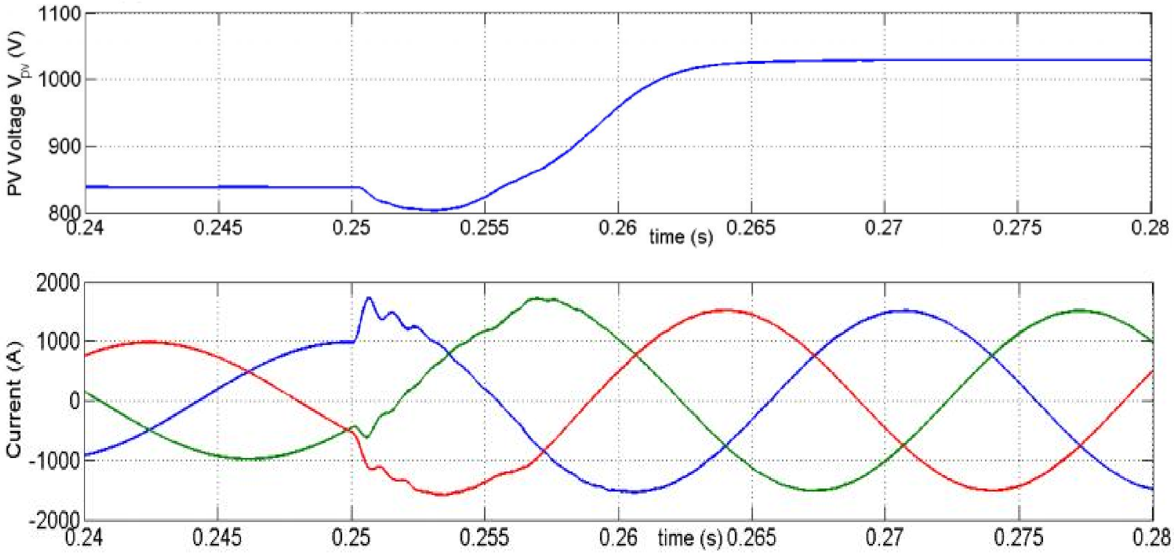

Figure 4.19: Transient portion of PV system DC bus voltage and current during fault

Concluding remarks are:

• To protect power electronic components and system, PV system output current limited to 1.5pu as shown in Figure 4.17.

• Fault requires reactive power, but PV generates active power. This active power must be dumped inside the capacitor which in-turn raises the capacitor voltage as shown in figure 4.18.

• Increased capacitor voltage leads to less PV current I_{pv} and power P_{pv} (refer the PV cell characteristic) as shown in figure 4.18.

• During fault, DC bus voltage is decided by power flow and MPPT has less control over DC bus capacitor voltage. So MPPT won't affect ton dynamics of the system during fault condition.

• At the instant of fault, the response of the PV depends on controller design, (PWM) technique and DC bus capacitor.

CHAPTER FIVE

CONCLUSION AND RECOMMENDATIONS

5.1 Conclusion

• System with voltage controller showing better performance. Voltage controller reducing the effect of the MPPT during the grid voltage disturbances.

• MPPT acts an important role, during large DC voltage disturbances under non-fault conditions. It has less effect on dynamics of the system during three phase fault condition.

• PLL dynamics act as a very important role in non fault grid disturbances (voltage and frequency disturbances), it has very less influence on system response, during climatic disturbances.

• PV system fault current is limited between 1.5 to 2pu, so PV panel contribution to the system fault is very less (depends on the penetration level).

• MPPT acts as an important role in system dynamics during climatic disturbances. MPPT have much effect during absence of voltage controller, large climatic disturbance and system with high PV penetration.

• Current and voltage controller have effect in system dynamics during all possible grid and climatic disturbances. Current controller bandwidth is depends on the filter inductance (which act as a plant) and PI controller.

• Change in controller parameter affects the transient response of the system during fault, faster controller have less fault current overshoot and slower controller have high fault current overshoot. Saturation block (Limit) in the PI controller also affects the transient response of the PV system.

• Transient response of the PV system is depends on the design parameters (like controller, filter design, DC bus Capacitor). So it is not possible to standardize the transient response of the system.

• MPPT is helping the system to reach stable condition.

5.2 Recommendations

The following recommendation are made for future research

- This thesis considered balanced loading of feeders and multiple PV panels of same size connected to network. A similar fault study carried out on test network with unequally loaded phases and equal penetration level of PV in each phase may be performed to acquire better understanding of the problem.
- In this thesis various grid and climatic disturbances have been investigated, other disturbances like grid- islanding disturbances must be including in future work.
- Results analyzing and processing in this project was done by (MATLAB simulation) program, the same results could be processed using by other programs like PSCAD and comparing results.

REFERENCES

[1] Brazilian, M. Oneyeji, I. Liebreich, M. Macgill, I. Chase, J. Gielen, D. Arent, D. Landfear, "Re-considering the Economics of Photovoltaic Power", Renene, 2012.

[2] Zeineldin. H.H, El-Saadany. Ehab F, Salama. M.M.A "Impact of DG Interface Control on Islanding Detection and Nondetection Zones", IEEE Transactions on Power Delivery, Vol. 21, No.3, July 2006.

[3] Yun Tiam Tan, "Impact on the Power System with a Large Penetration of PV Generation",PhD. Thesis, Dept. of Electrical Engineering and Electronics, UMSIT, February 2004.

[4] Castaner, Luis, Silvertre, Santiago, "Modelling of Photovoltaic System using PSpice", John Wiley and sons Ltd, September 2002.

[5] Tiam Tan.Y, Kirschen. D.S, Jenkins. N, "A Model of PV Generation Suitable for Stability Analysis", IEEE Transactions on Energy Conversion, November 2004.

[6] Bke Ulrich, "A Simple Model of Photovoltaic Module Electric Characteristics", Philips Research, Germany, 2008.

[7] M. E. Ropp and D. P Hohm, "Comparative Study of Maximum Power Point Tracking Algorithms Using an Experimental, Programmable, Maximum Power Point Tracking Test Bed", IEEE Photovoltaic Specialists Conference, Anchorage, AK, USA, 2000.

[8] Anirban Ghosal, Dr. Vinod John, "A Method to Improve PLL Performance Under Abnormal Grid Conditions", NPEC, 2007.

[9] Sidhu T.S, Bejmert D, "Short-Circuit Current Contribution from Large Scale PV Power Plant in the Context of Distribution Power system Protection ", IET Conference on RPG, Sept. 2011.

[10] A. Girgis and S. Brahma,"Effect of Distributed Generation on Protective Device Coordination in Distributed Systems", IEEE Conference on Power Engineering LESCOPE, Halifax, Canada, PP. 115-119, 11th to 13th July, 2001.

[11] S. Chaitusaney and A. Yokoyama, "Impact of Protection Coordination on Sizes of Several Distributed Generation Sources", IEEE Conference on Power Engineering,Singapore, Vol-2, PP. 669-674, 29th Nov to 2nd Dec, 2005.

[12] S. Chaitusaney and A. Yokoyama "An Appropriate Distributed Generation Sizing Considering Recloser-Fuse Coordination", IEEE Conference on Transmission and Distribution, Asia and Pacific, Dalian, China, 2005, Pages 1-6.

[13] S. Chaitusaney and A. Yokogama, "Prevention of Reliability Degradation from Recloser –Fuse miscoordination due to Distributed Generation," IEEE Transactions on Power Delivery, Vol 23, Issue 4, PP. 2545-2554, 2008.

[14] B. W. El-Khattam and T. S. Sidhu, "Restoration of Directional Overcurrent Relay Coordination in Distributed Generation System Utilizing Fault Current Limiter", IEEE Transactions on Power Delivery, Vol 23, Issue 2, PP. 576-585, 2008.

[15] D. Turcotte and F. Katiraei, "Fault Contribution of Grid Connected Inverters", IEEE conference on Electrical Power and Energy, Montreal, Canada, PP. 1-5, 22nd Oct to 23rd Oct, 2009.

[16] Mesut E Baran and Esmail El Markaby, "Fault Analysis on Distribution Feeders with Distributed Generators", IEEE Transactions on Power Systems, Vol 20, Issue 4, PP. 1757-1764, 2005.

[17] Cahier Techinque, “Calculation of short circuit currents”, Schneider Electric corporation, No.158, 2005.

APPENDIX A

MATLAB/SIMULINK MODEL

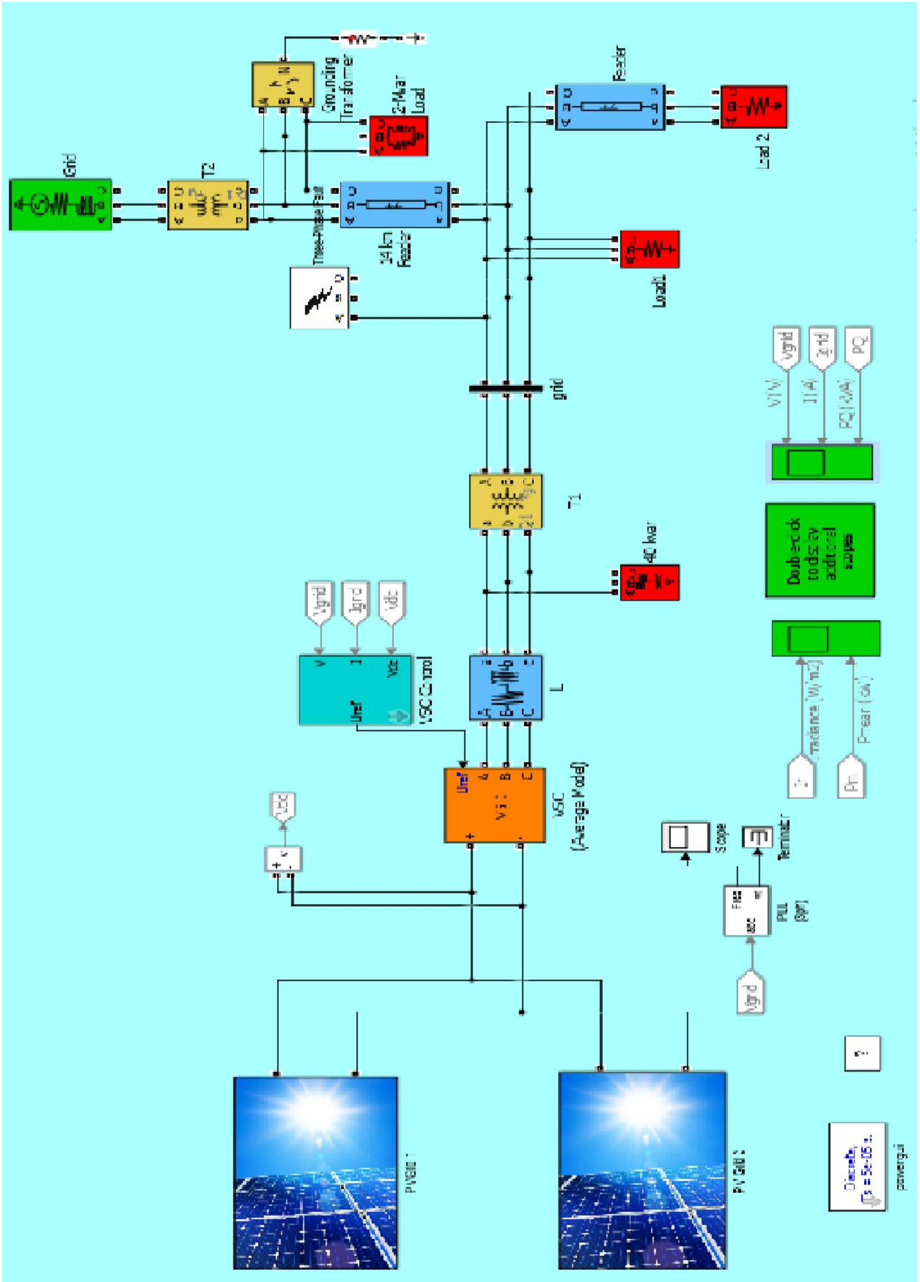

Figure A.1: Overall MATLAB/SIMULINK model

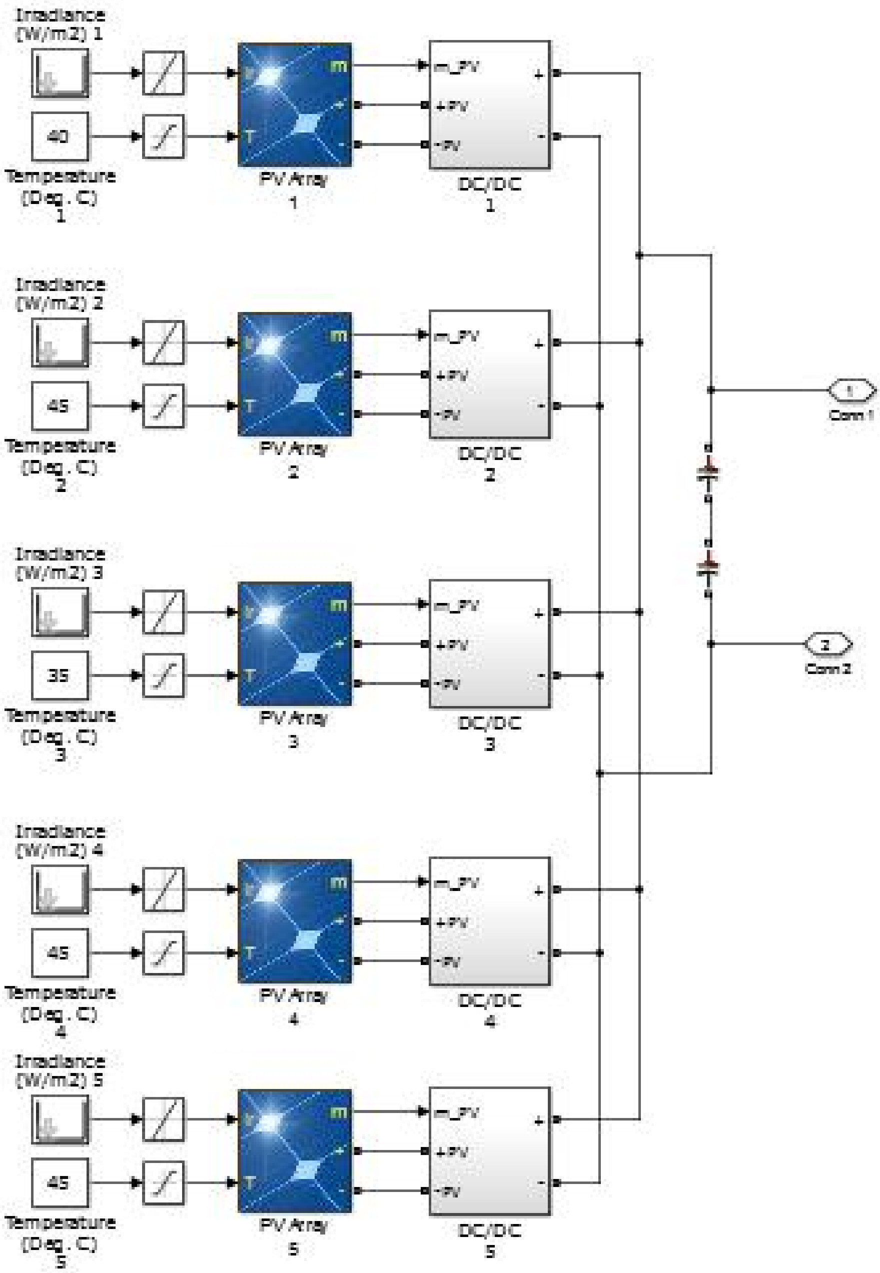

Figure A.2: Single PV grid subsystem

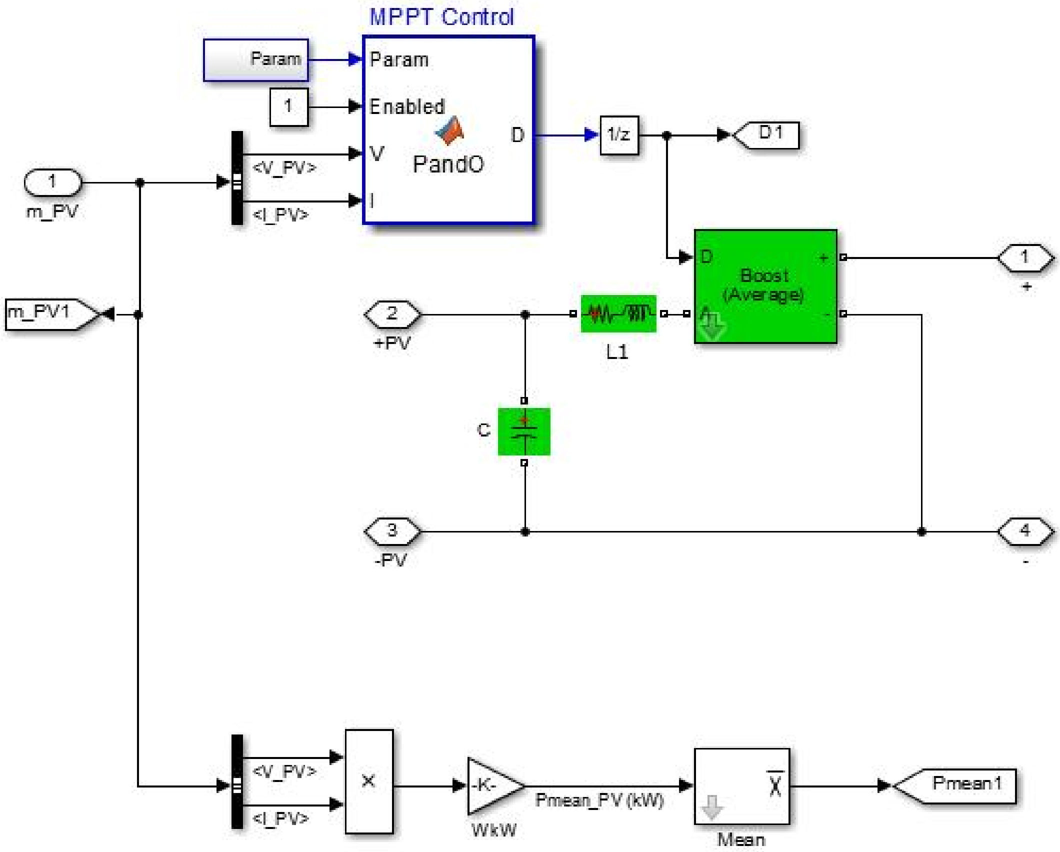

Figure A.3: DC-DC convertor subsystem

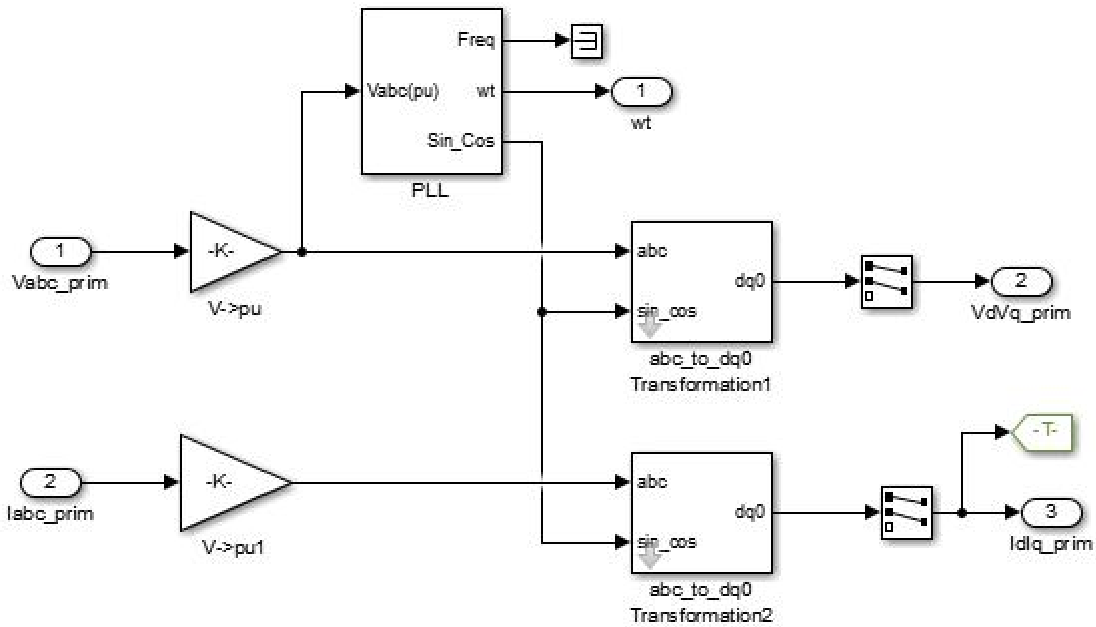

Figure A.4: PLL subsystem

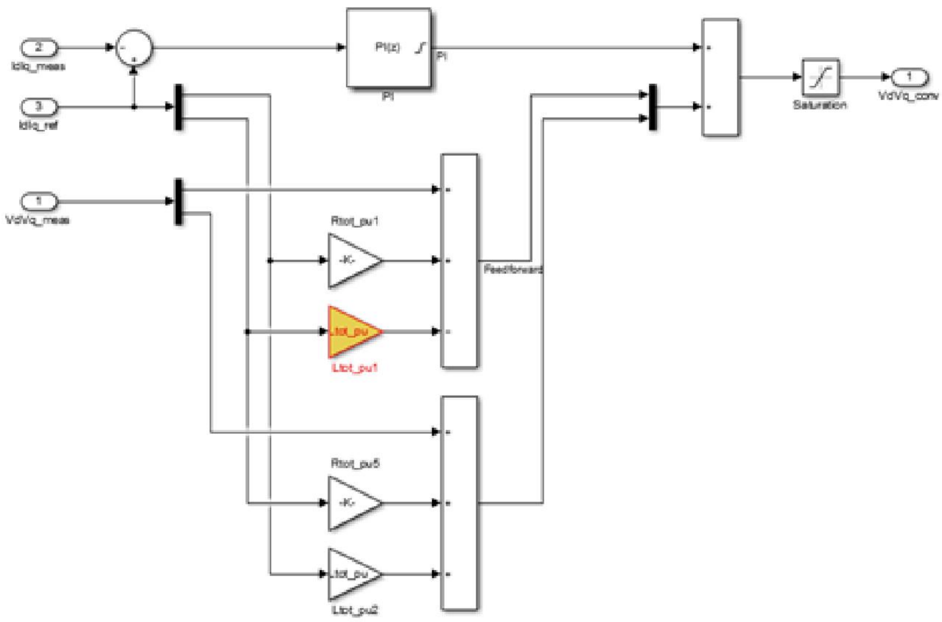

Figure A.5: Current controller subsystem

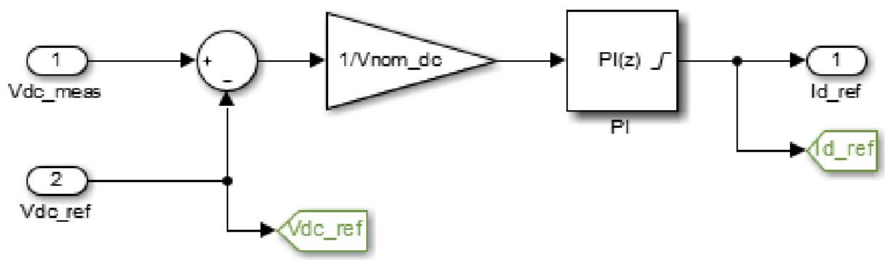

Figure A.6: Voltage controller subsystem

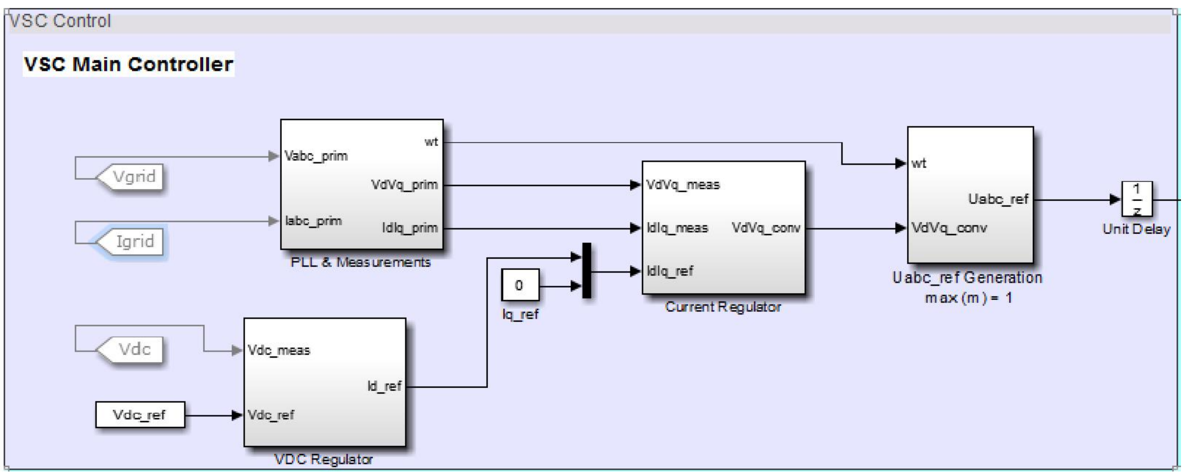

Figure A.7: VSC control subsystem

APPENDIX B

MANFACTURAL DATA

Table B.1: Electrical specification

Model	HIT Power 215A or HIT-N215A01
Rated Power (Pmax)[1]	215 W
Maximum Power Voltage (Vpm)	42.0 V
Maximum Power Current (Ipm)	5.13 A
Open Circuit Voltage (Voc)	51.6 V
Short Circuit Current (Isc)	5.61 A
Temperature Coefficient (Pmax)	-0.336%/ °C
Temperature Coefficient (Voc)	-0.143 V/ °C
Temperature Coefficient (Isc)	1.96 mA/ °C
NOCT	114.8°F (46°C)
CEC PTC Rating	199.6 W
Cell Efficiency	19.3%
Module Efficiency	17.1%
Watts per Ft.[2]	15.85 W
Maximum System Voltage	600 V
Series Fuse Rating	15 A
Warranted Tolerance (-/+)	-0% / +10%

Table B.2: Mechnical specification

Internal Bypass Diodes	3 Bypass Diodes
Module Area	13.56 Ft^2 (1.26m^2)
Weight	35.3 Lbs. (16kg)
Dimensions LxWxH	62.2x31.4x1.8 in. (1580x798x46 mm)
Cable Length +Male/-Female	46.45/40.55 in. (1180/1030 mm)
Cable Size / Connector Type	No. 12 AWG / MC4™ Locking Connectors
Static Wind / Snow Load	60PSF (2880Pa) / 39PSF (1867Pa)
Pallet Dimensions LxWxH	63.2x32x72.8 in. (1607x815x1850 mm)
Quantity per Pallet / Pallet Weight	34 pcs./1234.5 Lbs (560 kg)
Quantity per 53' Trailer	952 pcs.

Table B.3: Operating conditions and safety ratings

Ambient Operating Temperature	-4°F to 115°F (-20°C to 46°C)[2]
Hail Safety Impact Velocity	1" hailstone (25mm) at 52 mph (23m/s)
Fire Safety Classification	Class C
Safety & Rating Certifications	UL 1703, cUL, CEC
Limited Warranty	5 Years Workmanship, 20 Years Power Output
[1]STC: Cell temp. 25°C, AM1.5, 1000W/m² [2]Monthly average low and high of the installation site. Note: Specifications and information above may change without notice. All modules connected in the solar array should be of the same model number.	

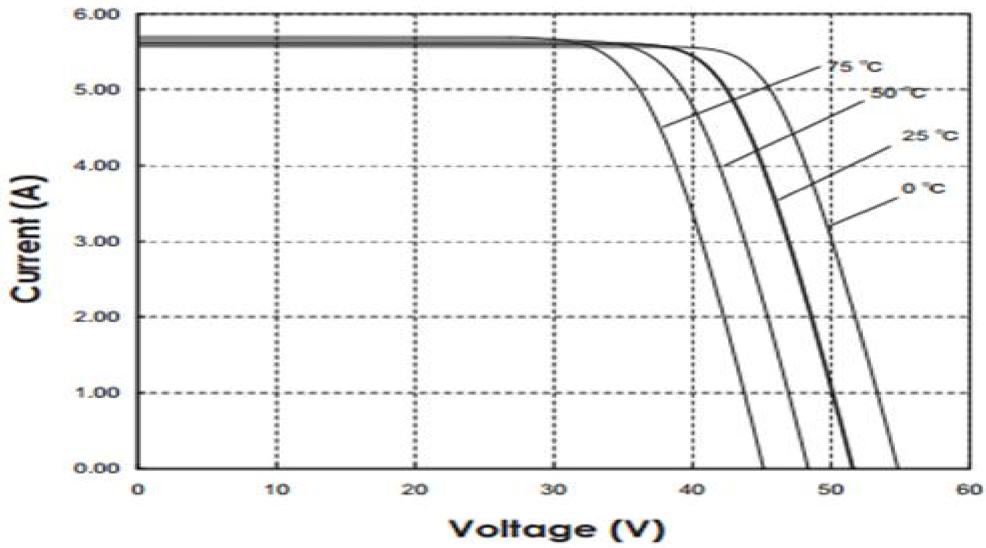

FigureB.1: Dependance on temperature

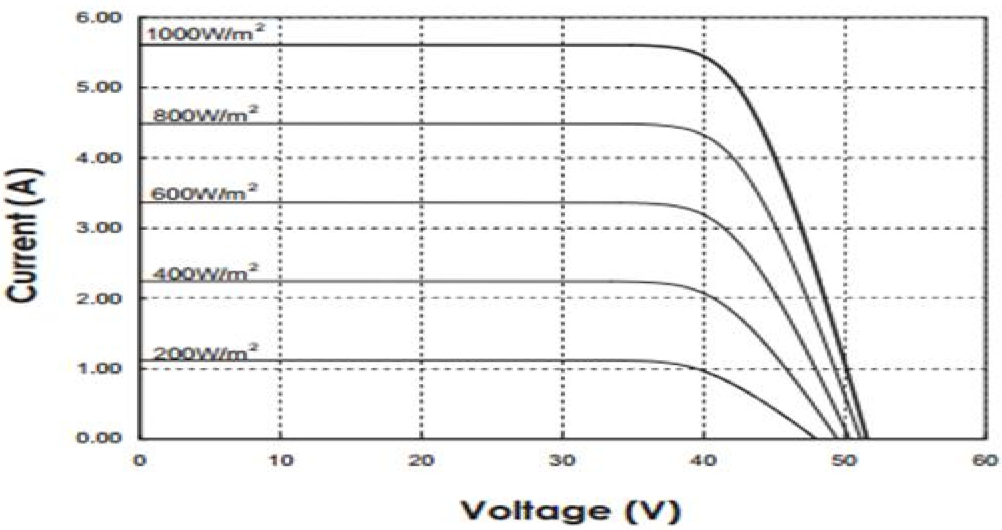

FigureB.2: Dependance on irradiance

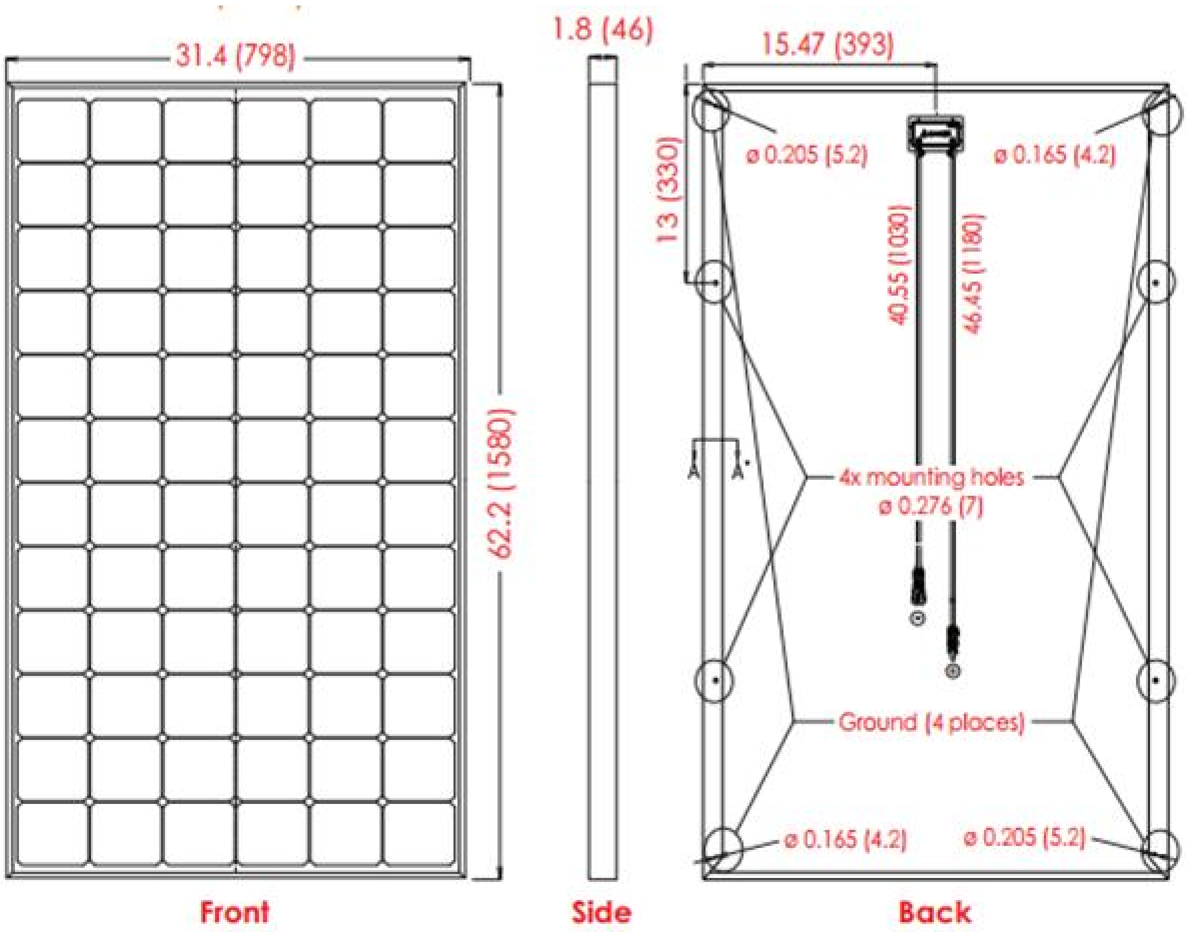

FigureB.3: Dimensions in inches